



UNIVERSITÀ POLITECNICA DELLE MARCHE

Facoltà di Ingegneria

Corso di Laurea Magistrale in Biomedical Engineering

**DEVELOPMENT OF A REHABILITATION EXERCISE FOR ASSISTED GRASPING THROUGH
COLLABORATIVE ROBOT**

Supervisor:

Dr. Giacomo PALMIERI

Co-Supervisor:

Dr. Luca CARBONARI

Dr. Giorgia CHIRIATTI

Author:

Luca APOLLONIO

A.A. 2021/2022



UNIVERSITÀ POLITECNICA DELLE MARCHE

Facoltà di Ingegneria

Corso di Laurea Magistrale in Biomedical Engineering

**DEVELOPMENT OF A REHABILITATION EXERCISE FOR ASSISTED GRASPING THROUGH
COLLABORATIVE ROBOT**

Supervisor:

Dr. Giacomo PALMIERI

Co-Supervisor:

Dr. Luca CARBONARI

Dr. Giorgia CHIRIATTI

Author:

Luca APOLLONIO

A.A. 2021/2022

Acknowledgments

One thought is for my family, who accompanied me throughout the journey. One to my love, who gave me the strength day by day to face obstacles. One to my friends, who shared anxiety and joy with me.

And finally, A thank you goes to the whole group of mechanical engineering department, who helped me throughout the work and accompanied me to the end of the journey.

Thank you all.

Abstract

In terms of safety, mobility, and programmability, collaborative robots constitute a progression of industrial robots. These qualities encourage the employment of these robots in the medical industry, including their use in neuromuscular rehabilitation, in addition to industrial uses. The research on robot-based rehabilitation therapy is leading to the growth of factors including the aging of the world population and technological advancements in healthcare. The rise of cobots causes increase in Human-Robot Interaction (HRI), where the functional involvement of humans has become an integral part of the design process of both robots and applications. To overcome the limitations of the traditional therapy, these years, the use of robot-assisted rehabilitation is rising. Robot-assisted therapy offers the possibility of increasing the intensity and duration of rehabilitation, enhancing the benefits of the therapy. The first cobot developed for the rehabilitation purposes as been the REHAROB. From this example, several other machines were developed, like the ARMEO robots, the MIME for upper-limb rehabilitation, the Motion Maker and the Walk Trainer. In our days industrial anthropomorphic robots such as Universal Robot (UR) robots and KUKA are employed in rehabilitation of lower and upper limbs.

The aim of this study is the development of a rehabilitation exercise for assisted grasping through the UR5e robot. The exercise is based on the end-effector connection between robot and the human hand. The purpose is to reach a target with the hand, following a planned trajectory computed by the robot itself from one point to another, then grab and release the target and repeat. The project evolved following several steps. A specific handle was modeled and printed for use in the experiment. After that, starting from an exercise that was already analyzed, a control law was developed to help arm rotation during the exercise. Impedance control and a force law appended during the performance of the exercise were also developed. The exercise is divided into three modes with different difficulties, where the feature that varies is the force generated by the robot along the trajectory, which can help or resist the movement toward the target.

To validate the exercise, data were acquired from ten subjects. Analyses of the data are based on the error given by the actual trajectory compared with the planned one, the characteristics expressed by the force recorded during the exercise, and the correlation coefficient between force and trajectory. From the trajectory results, it can be established that the highest mean error (\pm std) is produced during the easy modality (0.0428 ± 0.02 m). From the force analysis, it can be observed that the highest average human force registered by the Tool Centre Point (TCP) during the exercise is produced in medium mode with a value of 20.38 ± 9.71 N on the right arm. The goal of the thesis has been completed, furthermore, this work can be further pursued in the future by working on the modes of exercise.

Contents

Abstract	7
Chapter 1	14
1.1. Collaborative Robots	14
1.2. The importance of rehabilitation practice	16
1.3. Robot in Rehabilitation.....	17
1.3.1. Rehabilitation robots' categories	17
1.4. State of art of robots in rehabilitation	19
Chapter 2	22
2.1. UR5 in rehabilitation	22
2.2. Layout.....	25
2.3. Custom Handle	27
Chapter 3	32
3.1. Control Laws	32
3.1.1. Wrist Law	32
3.1.2. Impedance Control Law	35
3.1.3. Robot Force	35
3.2. Rehabilitation Exercise.....	36
3.3. Data Acquisition.....	38
3.4. Data Processing	39
Chapter 4	40
4.1. Results from the control law.....	40
4.2. Results from the rehabilitation exercise	44
4.2.1. Trajectory results	44
4.2.2. Force results.....	61
Chapter 5	67
5.1. Discussion.....	67
5.2. Conclusion.....	69
Bibliography	70
Appendix A	75

List of Figures

Figure 1.1.: Human-Robot Interaction [5].	15
Figure 1.2.: a) End-effector robot. b) Exoskeleton robot.	18
Figure 1.3.: MIT-Manus robot for upper limb rehabilitation [39].	19
Figure 1.4.: Evolution of rehabilitation robots.	20
Figure 2.1.: Universal Robot family, from left to right: UR3, UR5, UR10.	22
Figure 2.2.: UR5e structure.	23
Figure 2.3.: UR5e components. a) Control Unit. b) Teach pendant.	24
Figure 2.4.: Experiment Layout.	26
Figure 2.5.: Exercise Target used during the rehabilitation exercise.	26
Figure 2.6.: Cognex 2D camera.	27
Figure 2.7.: Custom handle sketches.	27
Figure 2.8.: Custom handle prototypes in rhinoceros.	28
Figure 2.9.: The custom handle that has been chosen.	29
Figure 2.10.: Custom lock system.	29
Figure 2.11.: Perspective views of the custom handle.	30
Figure 2.12.: Form 3+ 3D printer.	30
Figure 2.13.: The custom handle components.	31
Figure 3.1.: Representation of the control law.	34
Figure 3.2.: Simulink model.	34
Figure 3.3.: Exercise configuration.	36
Figure 3.4.: Working table.	37
Figure 3.5.: Target positions during the exercise.	38
Figure 4.1.: Comparison between the control laws and the freedrive.	41
Figure 4.2.: Comparison between the control laws and the freedrive with no inputs.	42
Figure 4.3.: Control law relationship with the angle of rotation.	43
Figure 4.4.: Easy mode. a) All actual TCP trajectories of right arm. b) All planned TCP trajectories of right arm.	45
Figure 4.5.: Easy mode. a) All actual TCP trajectories of left arm. b) All planned TCP trajectories of left arm.	45
Figure 4.6.: Medium mode. a) All actual TCP trajectories of right arm. b) All planned TCP trajectories of right arm.	46
Figure 4.7.: Medium mode. a) All actual TCP trajectories of left arm. b) All planned TCP trajectories of left arm.	46
Figure 4.8.: Hard mode. a) All actual TCP trajectories of left arm. b) All planned TCP trajectories of left arm.	47
Figure 4.9.: Hard mode. a) All actual TCP trajectories of left arm. b) All planned TCP trajectories of left arm.	47
Figure 4.10.: Easy mode. a) All planned and actual TCP trajectories of left arm. b) All planned and actual TCP trajectories of left arm.	48
Figure 4.11.: Medium mode. a) All planned and actual TCP trajectories of left arm. b) All planned and actual TCP trajectories of left arm.	49
Figure 4.12.: Hard mode. a) All planned and actual TCP trajectories of left arm. b) All planned and actual TCP trajectories of left arm.	50

Figure 4.13.: Right arm trajectories of Subject 0..... 51
Figure 4.14.: Right arm trajectories Subject 0.52
Figure 4.15.: TCP force recorded on X, Y and Z axis during one repetition in easy mode. 61
Figure 4.16.: TCP force recorded on X, Y and Z axis during one repetition in medium mode.62
Figure 4.17.: TCP force recorded on X, Y and Z axis during one repetition in hard mode. 62

List of Tables

Table 1.1.: Technical specifications UR5e.	23
Table 4.1.: Results from the comparison of the two control laws.....	44
Table 4.2.: Distance between the actual and planned trajectory for each subject in easy mode. R and L represents Right arm and Left arm. RMSE is the Root Mean Square Error.	54
Table 4.3.: Distance between the actual and planned trajectory for each subject in medium mode. R and L represents Right arm and Left arm. RMSE is the Root Mean Square Error.	55
Table 4.4.: Distance between the actual and planned trajectory for each subject in hard mode. R and L represents Right arm and Left arm. RMSE is the Root Mean Square Error.	56
Table 4.5.: Mean error \pm standard deviation of trajectory for all the subjects.	57
Table 4.6.: Correlation factor between trajectory and TCP force during exercise in easy mode.	58
Table 4.7.: Correlation factor between trajectory and TCP force during exercise in medium mode.	59
Table 4.8.: Correlation factor between trajectory and TCP force during exercise in hard mode.	60
Table 4.9.: Results from the force analysis in easy mode. The force is analysed in its Mean, Median, Maximum and Minimum value.	63
Table 4.10.: Results from the force analysis in medium mode. The force is analysed in its Mean, Median, Maximum and Minimum value.	64
Table 4.11.: Results from the force analysis in hard mode. The force is analysed in its Mean, Median, Maximum and Minimum value.	65
Table 4.12.: Mean, Median, Minimum and Maximum force value and Standard Deviation on all subject in easy, medium, and hard mode.	66

List of Equations

Equation 3.1. cubic polynomial control law.	33
Equation 3.2. Manipulator dynamics equation.	33
Equation 3.3. Spring-like equation.	35

Chapter 1.

Introduction

Collaborative robots arise as an evolution of industrial robots in terms of safety, lightweight, and programmability. These characteristics lead to the adoption of these robots not only for industrial applications but also in the medical field, including their use in neuromuscular rehabilitation. Factors such as the ageing of the global population, and technological development in health care, increase the research on robot-based rehabilitation therapies. The aim of this thesis project is based on the development of a new neuromuscular rehabilitation exercise for the upper limb, using a collaborative robot. The framework of the exercise is constructed in such a way as to allow freedom of movement for the fingers, allowing the grasping of a target during the rehabilitation.

1.1. Collaborative Robots

The idea of collaborative robots, also known as cobots, was born from a General Motors initiative, in 1994, led by Prasad Akella. In 1996 the concept was developed by the revolutionary professors, J. Edward Colgate and Michael Peshkin, both professors at North-western University. The initial vision at the base of their project, which was later developed with the writing of a US patent entitled “Cobots” [1], was to create a robot that allows the direct physical interaction between a person and a multitasking manipulator through computer control.

Collaborative robots were developed to execute tasks side by side with the human workforce, meanwhile sharing the same working spaces, offering high performances without the need for advanced programming skills [2]. The main idea of collaborative robotics is the empowering and the assisting of humans during certain tasks that cannot be accomplished by other solutions, without the use of a robot. Thus, increasing the benefits of humans during tasks.

The rise of cobots has resulted in a consequent increase in robot-human relationships, where the functional involvement of humans has become an integral part of the design process of both robots and applications, called as Human-Robot Interaction or Human-Robot Interface (HRI) (Fig. 1.1). Thus, providing increased productivity with reduced production costs by combining principal characteristics of both sides.

In detail, it is defined as physical Human-Robot Interaction (pHRI) any physical interaction between humans and robots to perform an independent or cooperative task in the same working area, by guaranteeing determined performances in terms of safety and human ergonomics.[3] However, various challenges still need to be addressed for what concerns the interaction modalities, like gaze, speech or gestures, that need to be formalized to be interpreted in the right way by robot control algorithms, and all the disambiguates need to be fixed. [4]

To increase the efficiency of Human-Robot collaboration compared with the human standalone work, a robot must be able to mimic human behaviour, performing both active and passive parts of the

interaction. Thus, combining the strength, precision and endurance of mechanical robots with the flexibility, dexterity and problem-solving skills of human workers. [2]

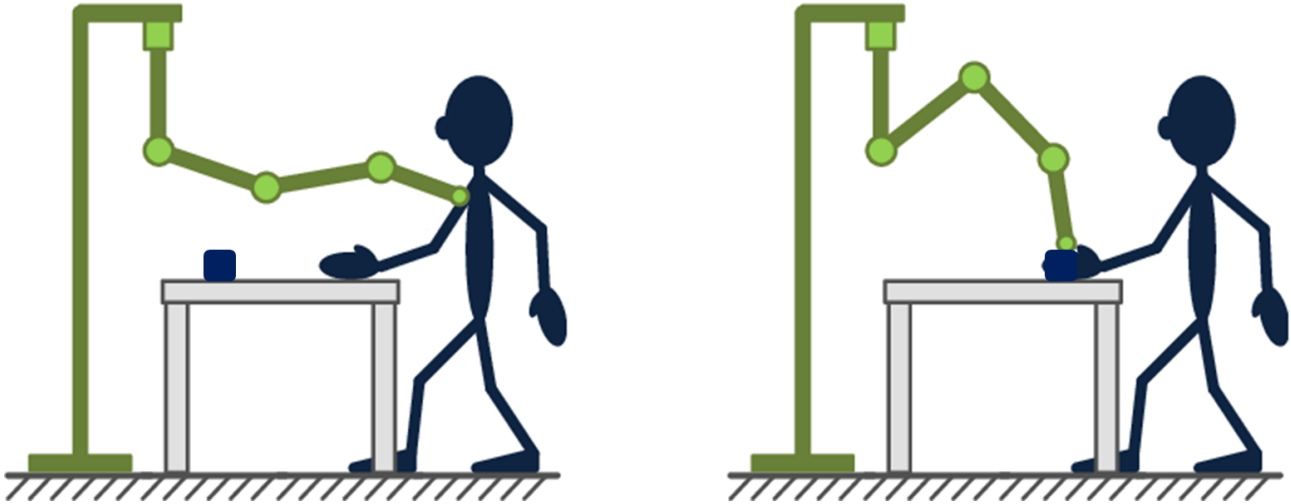


Figure 1.1.: Human-Robot Interaction [5].

One of the main features of cobot is their capabilities to be easily programmed by every worker, even without a strong programming background. Moreover, it includes a hand guiding feature, where a user can teach the robot to follow specific trajectories. Another major benefit that Cobots offer is their already incorporated safety features. Indeed, they have very low inertia forces, and force/torque sensors implemented on each joint to detect any kind of external impact. Thus, Safety in collaborative robotics is stated as a non-negotiable aspect in the design of a robot system [6], i.e. each Cobot is equipped with a sensor-based stop monitoring system, which provides an instantaneous stop of the robot's movement if a human has entered the operational or collaborative work area.

Although industrial robots have played a vital role within the automotive industry and its suppliers, their high cost, large size, weight, and sophisticated programming requirements have limited their use in other vertical industries. Compared with the already established industrial robots, cobots offer increased flexibility, versatility, and productivity, without sacrificing safety systems. The lightweight structure of these robots offers great mobility, in terms of both transportation and work, something that is lacking in their industrial counterparts, due to their massive structure. Finally, they are easily programmable, offering great computing capabilities without hard coding them.

Due to their capabilities, collaborative robots have been firstly involved in the industry environment, as an assistant to the worker, speeding up and automating previously ignored tasks. Subsequently, thanks to the structural advantages and adaptability in different situations, their use has increased in many other fields of work, one of which is the medical field, where the Cobot is used to carry out or help doctors in performing complex surgical tasks and, even more, as a therapeutic rehabilitation system to cooperate with patients.

1.2. The importance of rehabilitation practice

Nowadays, the field of rehabilitation is gaining more and more importance worldwide. This increase is due to factors such as the ageing of the global population, and technological development in health care, which result in the increase of both musculoskeletal and neurological diseases in the population. Before moving on, it is crucial to define the word “rehabilitation”. Following the definition from the World Health Organization (WHO) in the World Report of Disability in 2011, the rehabilitation is defined as ” a set of measures that assist individuals who experience, or are likely to experience, disability to achieve and maintain optimal functioning in interaction with their environments” [7].

An estimate of the need for rehabilitation is given by the 2019 Global Burden of Disease study, where parameters such as prevalence and Years of Life with Disability (YLDs) are computed, analysed and sectorized according to different diseases [8]. Worldwide, from 1990 to 2019, the number of people in a condition that would benefit from rehabilitation therapy increased by 63%, reaching 2.41 billion individuals in 2019, with a YLDs of 310 million. In detail, the disease area that contributed most to prevalence was musculoskeletal disorders with 1.71 billion people. Furthermore, 255 million individuals with neurological disorders had conditions that would benefit from rehabilitation therapies, with 51 million in YLDs. From 1990 to 2019 these data increased by 104%. [8].

The most common cause of adult disabilities is given by stroke [9], a neurological disease belonging to the neurological disorder field. In detail, the ischemic stroke occurs if the blood supply in a part of the brain is reduced or interrupted, not allowing the correct perfusion and, as consequence, preventing the oxygenation of brain tissue [10]. In this case, brain cells begin to die in minutes, this causes different effects, depending on the brain area involved. Usually, the most affected area is the one that is involved in the control of movement and balance, providing the condition in which the individual affected by this disease needs rehabilitation. In detail, the affected area can produce a disability involving part or all the lower and upper limbs. For what concern the hand function, usually it is compromised after stroke, provoking an initial flaccid paresis that, gradually, results in a hypertonicity in both the flexo-extension [11].

The study by Kwakkel et al. analysed the limitation in the abilities of neural mechanisms to recover the missing functionalities after the stroke occurs and, it has been considered to reach a plateau in motor abilities related to the timing and the intensity of the stroke rehabilitation therapy [12].

In addition, studies by Buma et al. reported that the greatest gains that it is possible to achieve in motor function during rehabilitation, occur in the first-month post-stroke with additional improvements in the range of 6 months after the event [13].

Therefore, high-intensity rehabilitation therapy, organized by working on specific tasks, plays a crucial role in the recovery of all motor functions [14], [15]. Indeed, studies like [15]–[17] have stated that the repetition of specific movements during intensive treatments, has a good impact on the neuroplasticity and on the functional outcome improvement.

There are many types of rehabilitation therapies, depending on the area involved in the stroke and on the consequences of the post-stroke. From the lower to the upper limb, rehabilitation therapy is based on high-intensity task treatments.

Several works prove that arm therapy has increased the progress during the rehabilitation of stroke patients. [18], [19] The increase in motor function recovery and the improvement of movement coordination allow the subject to face with the Activities of Daily Living (ADLs), furthermore, prevent complications like the muscle atrophy, the spasticity and the joint degeneration [20].

1.3. Robot in Rehabilitation

Traditional rehabilitation therapy, based on manually assisted movement training, has many major limitations. The traditional rehabilitation is performed by a specialized therapist, which is under a continuous strain due to the high-intensity session, therefore, training duration is limited by the therapist's fatigue and not by the patient. Consequently, this condition leads to a reduction in the duration of training sessions, and as mentioned earlier, the recovery peak due to high-intensity therapy is less than expected. Another major limitation is the lack of inter-rater reliability and the low objectivity, both depending on the sensitivity of the therapist [20].

To overcome these limitations, in these years, the use of robot-assisted rehabilitation is rising. Robot-assisted therapy offers the possibility of increasing the duration and intensity of sessions, thus enhancing the productivity of rehabilitation [21], [22]. Another benefit is the contribution to the technological evolution of machines for muscular and cognitive training [23], [24], as well as their use in the assistance of subjects with low residual motor abilities.

Furthermore, this innovative form of rehabilitation enables the quantification of physical training, measuring the force, velocity, acceleration, and the Range of Motion (ROM) of a subject during the session, supporting the evaluation of the rehabilitation goals.

However, to enhance its benefits, fundamental is the adaptability of the robot system with respect to the human limb in terms of ROM, the number of degrees of freedom (DOFs) and in terms of segment size [20].

The use of robots in rehabilitation is additionally justified by the impact given on therapy outcomes, increasing the benefits of treatment and motor re-training, a crucial condition for a good recovery as well as the compensation [12], [25]–[27]. Based on the mechanisms of neurogenesis stimulated during training sessions [25], [28], [29], on the neuroplasticity, and the functional recovery [30], [31], emphasize the potential of these technologies in the field of rehabilitation.

1.3.1. Rehabilitation robots' categories

Rehabilitation robots can be organized in groups based on peculiar characteristics. One of which is mechanical structure, in which, they can be divided into end-effector and exoskeleton robots.

- End effector robotic systems exert forces in the most distal part of the structure, usually connected with the patient's forearm or hand (Fig.1.2a).
- Exoskeleton instead, allow determining the kinematic configuration of human joints (Fig.1.3b).

Both groups are used in robot-added therapy with equally great results.



Figure 1.2.: a) End-effector robot. b) Exoskeleton robot.

Another classification has been done in 2001, by Tejima [32] which characterized the type of rehabilitation robots based on their tasks. From his studies, four groups were developed:

- Augmentative robots, used to improve multiple tasks on the patient side.
- Augmentative mobility, used to improve patient mobility.
- Robots for help caregivers, used to help care-givers to accomplish tasks.
- Therapy robots, used in physical therapy.

Furthermore, from the fourth group, Badesa et al. [33] drew up a classification based on the support provided to the patient, providing two groups:

- Assistive mode, in which the robot generates forces that replace or add to the patient's ones.
- Resistive mode, where the robot produces forces to resist the patient's motion, meanwhile storing data about the performance.

From the latter classification, we should dwell on the fact that many studies have used an active assisted mode [34]. The preference is carried by the studies from Lynch et al, that, analysing high intensity continuous passive motion exercises, have demonstrated that it does not give any further advantage in the recovery of motor function [35], [36].

For what concern the type of rehabilitation therapy, also depends on the outcome of the stroke. Robotic rehabilitation was introduced essentially for upper and lower limbs recovery, even so, the upper limb rehabilitation is the most analysed [37]–[39]. Grosmaire et al., analysed the motor activity

of the upper limb during rehabilitation sessions. From the results, they have established that to have plastic changes and recover the limb, the session has to be planned with a high number of movement repetitions [36].

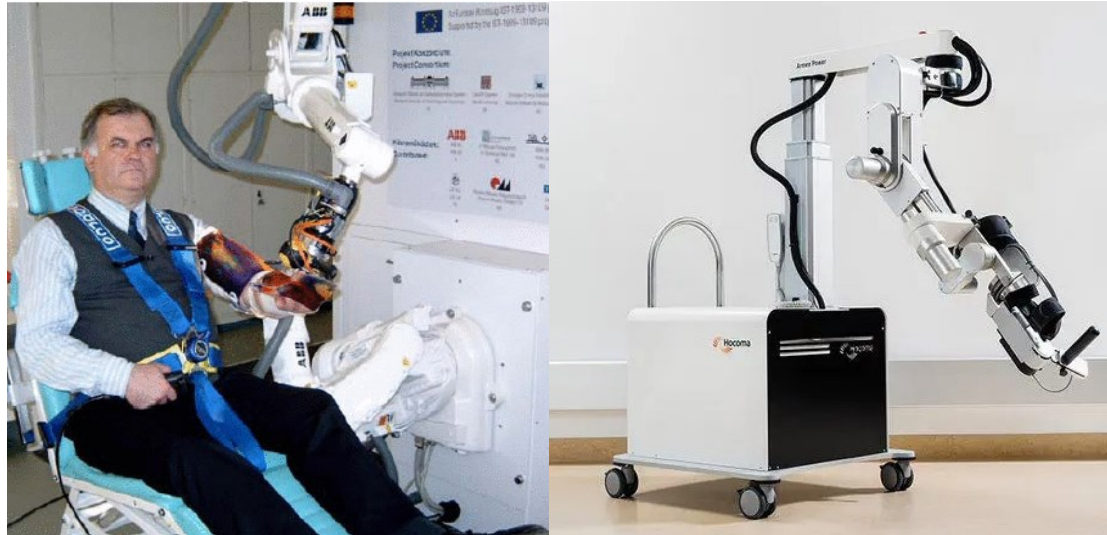
1.4. State of art of robots in rehabilitation

Since 1997, with the first clinical introduction of robots into the rehabilitation field, with the MIT-Manus robot [39] (Fig. 1.3.), the use of robot-added rehabilitation is increased.



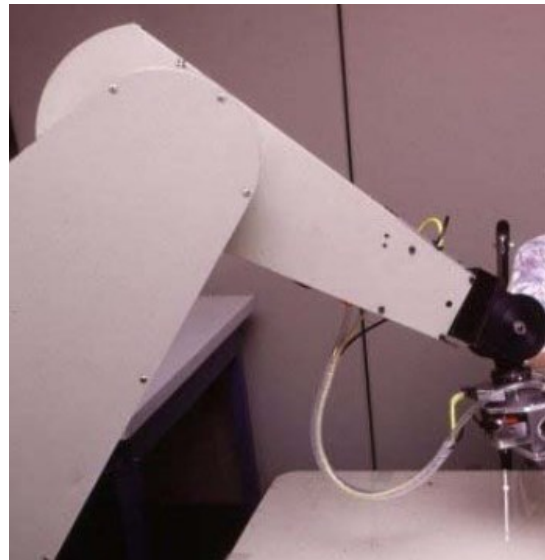
Figure 1.3.: MIT-Manus robot for upper limb rehabilitation [39].

In 1999, from the ideas developed by the Budapest University of Technology and Economics, is born an industrial robot used to perform a rehabilitation therapy, named REHAROB (Fig.1.4.a) [40]. From this example, several other machines were developed, like the ARMEO robots (Fig.1.4.b) [41], the MIME for upper-limb rehabilitation (Fig.1.4.c) [42], the Motion Maker and the Walk Trainer [43]–[45]. These last two robots were developed following the Cyberthosis concepts that combine mobilization and a closed-loop muscle electro-stimulation [46].



(a)

(b)



(c)

Figure 1.4.: Evolution of rehabilitation robots.

(a) REHAROB robot [40]. **(b)** ARMEO robot [41]. **(c)** MIME robot [42].

The literature is increasing the evidence of the efficiency of robot-based rehabilitation, producing great results in the reduction of impairment due to neurological diseases [47]–[52].

However, robotic interfaces were introduced in clinics, for arm and leg rehabilitation, with a focus on the upper limbs after stroke disability. To improve the efficiency of robot interfaces, the use of collaborative robots is increased.

Papaleo et al. [53], adapted the KUKA cobot with 7 Degree of Freedom (DOF), to the patient's real-time needs, attaching the subject to the end-effector of the robot and producing assistive force. The same was done by Prendergast et al.[54], that used KUKA in shoulder rehabilitation.

Fernandes [38] developed an intelligent robotic system for the rehabilitation of upper limbs using a UR3, connecting the arm to the end-effector of the robot. Chiriatti et al [55], presented a general framework for rehabilitation using the UR5e cobot from the Universal Robot. In [56] has been analysed the feasibility of the UR5 in the rehabilitation of upper limbs after stroke, producing good results.

Chapter 2.

2.1. UR5 in rehabilitation

The UR5 is a six-axis lightweight industrial manipulator, developed and produced by the Danish company Universal Robots. It is defined as collaborative robot thanks to its structural features such as flexibility, low speed, and high safety due to built-in controls, like the protective stop that act when an external force exceeds 150 N. It is part of the Universal Robot (UR) family, founded in 2005, that developed three types of robots respectively, UR3, UR5 and UR10 (Fig.2.1.). The name of each robot is an index of their payload capacity in kilograms. Thus, these cobots can be used in different industrial tasks and, depending on the type of work and on the load, the most suitable one can be chosen. In 2018, the Universal Robot company has produced the e-series (UR3e, UR5e, UR10e), made up with additional components and with a more versatile programming configuration. The UR5e complies with point 5.10.5 of the EN ISO 10218-1:2006 standard, thus enabling humans and robots to work in the same environment [56].



Figure 2.1.: Universal Robot family, from left to right: UR3, UR5, UR10.

UR5e is the perfect compromise in the automation of low-weight processing tasks, with a weight of 18.4 kg, a maximum payload of 5 kg and a maximum radius of 850 mm from the base joint. Each joint of the robot has a range of $\pm 360^\circ$, with a speed limit of each joint set to $\pm 180^\circ/s$ [57]. From Table 1.1 can be appreciated the technical specifications of UR5e designed for collaborative robot applications. If happens that safety limits are violated, the robot instantly stops, and the system enters in recovery mode. In recovery mode, the robot cannot be programmed and must be moved back to its limits.

Table 1.1.: Technical specifications UR5e.

Weight	18.4 kg
Payload	5kg
Reach	850 mm
Joint ranges	$\pm 360^\circ$
Speed	All joints: 180°/s. Tool: Typical 1 m/s.
Repeatability	± 0.1 mm
Footprint	$\varnothing 149$ mm
Degrees of freedom	6 rotating joints
Materials	Aluminium, PP plastic
Temperature	Work in a range of 0-50°C
Power supply	100-240 VAC, 50-60 Hz

The UR5e is composed of three parts:

- The Robot, which is an anthropomorphic type composed by 6 joints: Base, Shoulder, Elbow, Wrist 1, Wrist 2, and Wrist 3 (Fig.2.2.).
- The Control unit, which is the operative centre of the robot (Fig.2.3.a).
- The Teach Pendant (Fig.2.3.b), composed by a tablet, which allows the control of the robot with a Linux-based operative system and an Ethernet connection provided at the bottom of the control box.

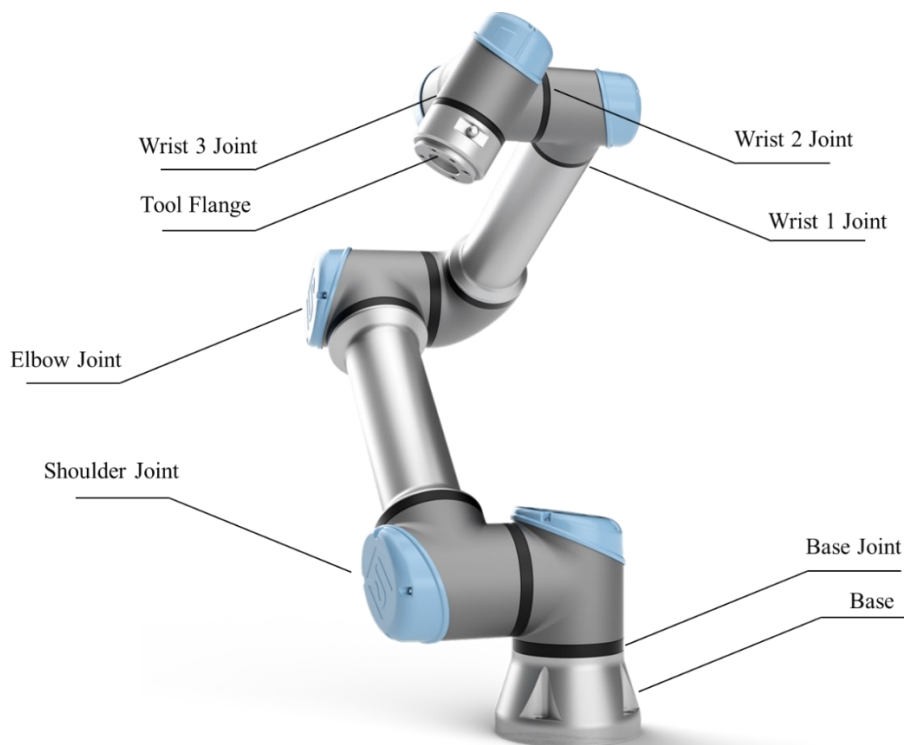


Figure 2.2.: UR5e structure.

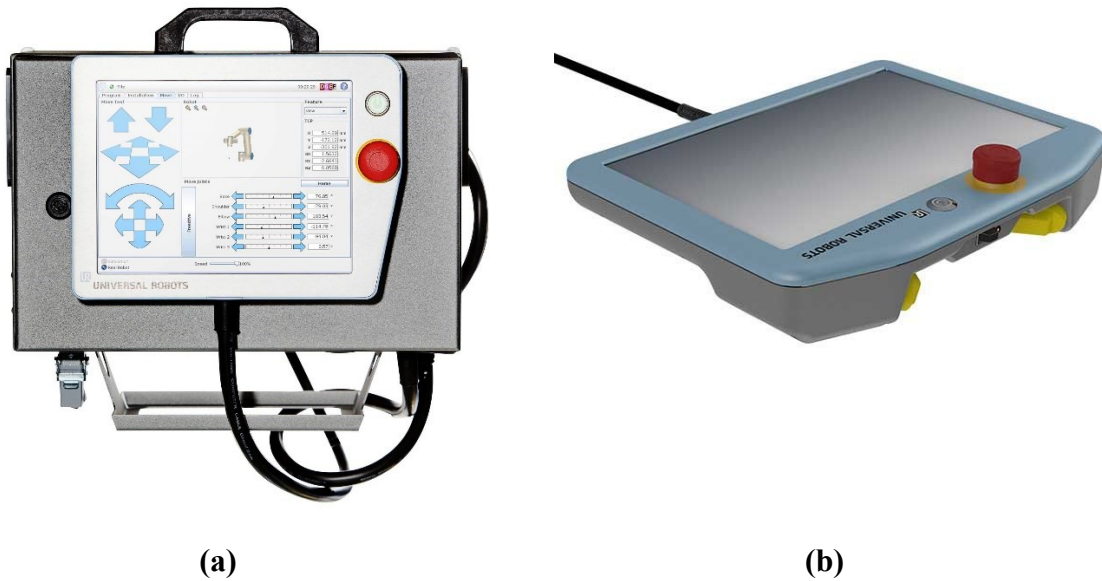


Figure 2.3.: UR5e components. **a)** Control Unit. **b)** Teach pendant.

The UR5e is empowered by its control box, connected to an input frequency of 47-63 Hz and an input voltage range of 100-240 VAC [57].

From the teach pendant it is possible to program the robot using the easy programming interfaces installed on it. Furthermore, it is possible to program directly with UR script language, developing remote script commands while the robot is running. It is possible to choose the programming environment spacing through C++, Phyton, Visual Basic or Java script.

The UR5e can be moved by means of four different methods:

- Speed command: making the robot move while maintaining a constant velocity.
- Servo command: the robot is moving toward the desired position and after all motions are blocked.
- Force command: the robot is compliant along one or more axes while moving along the others.
- Move command: the robot follows simple movements from one point to another.

Another way to move the robot is by means of the operator, using the self-learning modality, where the robot stores information to produce a planned trajectory.

The distinctive features of UR5 allow its use in various fields of work, ranging from the employment as an industrial manipulator, as grippers and in assembly operations, to the use in the medical and clinical fields as a rehabilitation robot. [55], [58], [59] The first attempts to use a Universal robot UR5 as an integral part of the rehabilitation framework was made by [60] implementing a set of reaching and grasping exercises. Later, UR5 was used in a rehabilitation framework as a replication of two simple 1 DOF training robots [61].

2.2. Layout

The experimental layout was based in the Department of Ingegneria Industriale e Scienze (DIISM) laboratories. Its representation is well provided in the Figure 2.4, by which all components are shown. The main component is the UR5e robot (1), a fundamental element of the experiment; then there is the custom handle (2), a 3D printed model connected at the Tool Centre Point (TCP), that allows the rehabilitation with grasping; the target (3), a custom cylindrical object (Fig.2.5.), used in rehabilitation exercise as grasping goal, it has a diameter of 52 mm and height of 51 mm ; the working table (4), a black table with a white rectangular area which constitutes the working area during the exercise. The Control Unit (5), a crucial point of the layout, from there the exercise is controlled at every point.

The exercise must be done in the predetermined working area, delimited by a white rectangle (53 cm x 34.5 cm). Where the working area is established using a Cognex 2D camera. The Cognex 2D vision system capture 2-dimension image, in various resolution, and allow to know time by time the position of the target during the exercise (Fig.2.6.). The working area is chosen by looking at the best resolution of the camera, so, the rectangular shaped area represents the space in which the Cognex 2D camera has its best resolution.

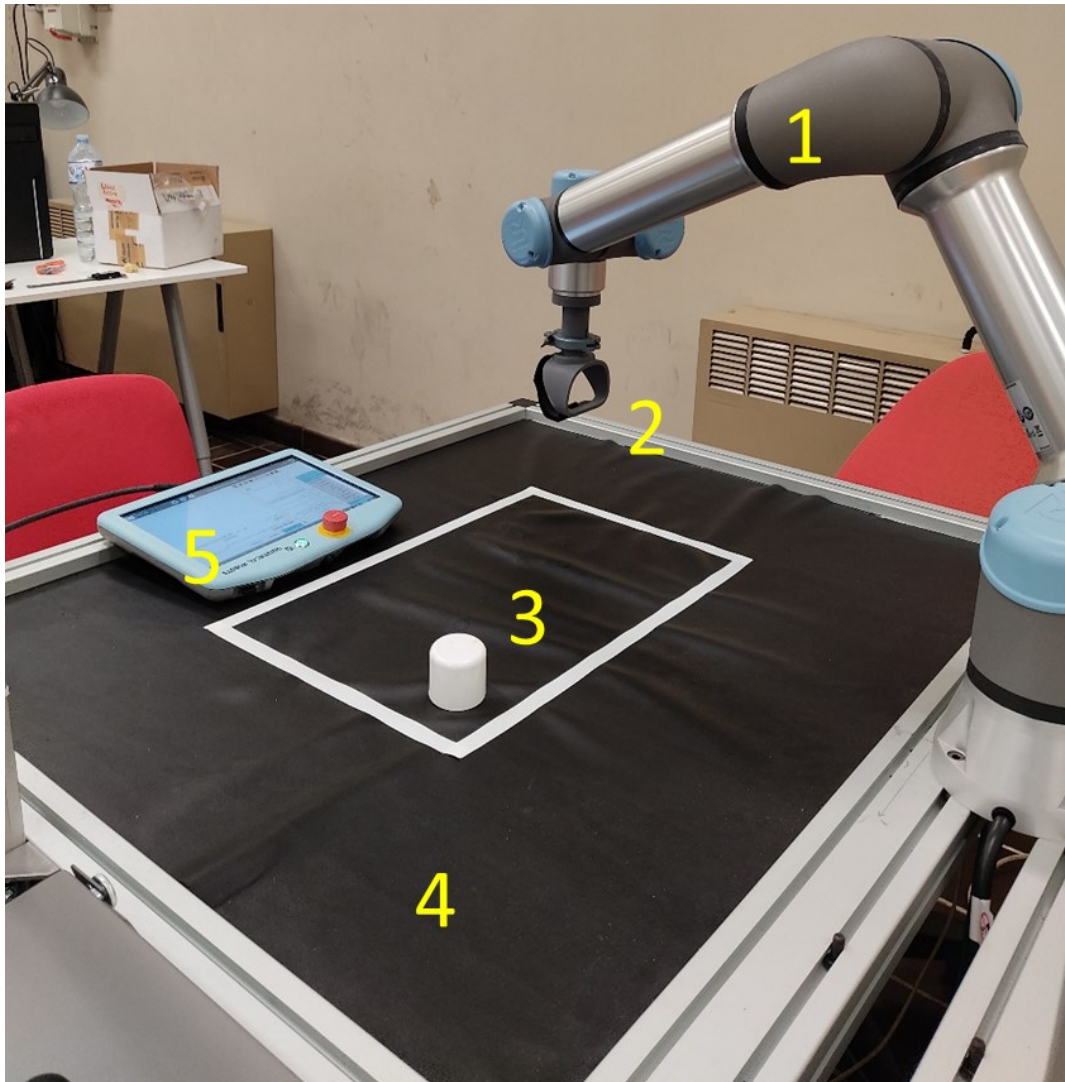


Figure 2.4.: Experiment Layout.

- 1) UR5e robot. 2) Custom made handle. 3) Exercise target. 4) Working table. 5) Tablet from control unit.



Figure 2.5.: Exercise Target used during the rehabilitation exercise.

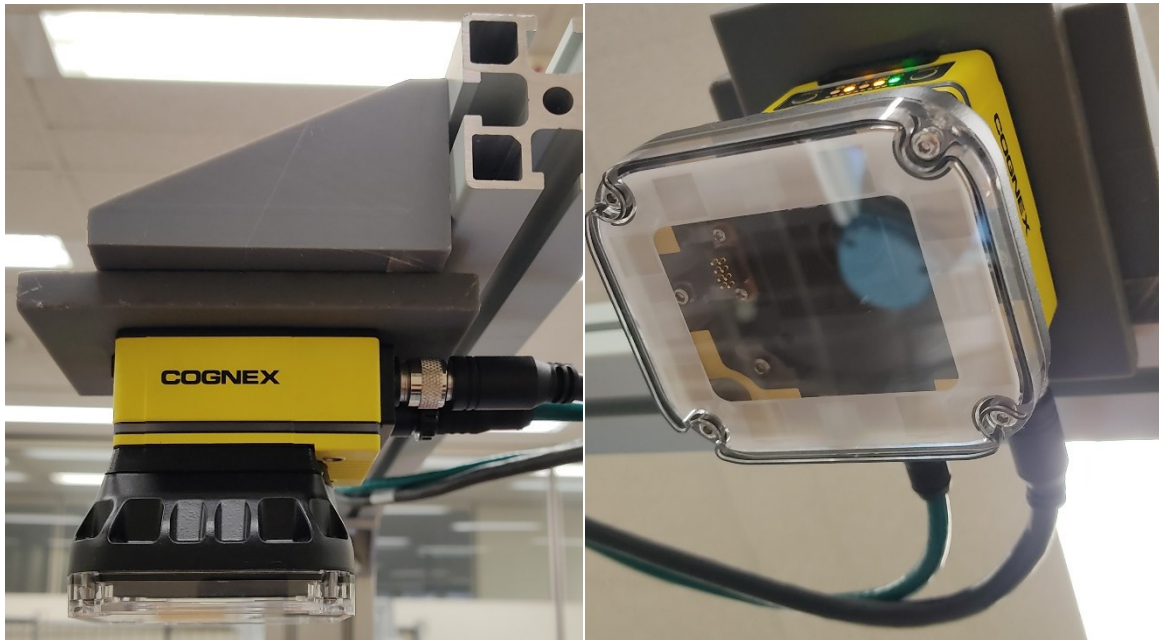


Figure 2.6.: Cognex 2D camera.

2.3. Custom Handle

The aim of this thesis is to create a rehabilitative exercise for the upper limb, which allows the free use of the hand, by which it is possible to grasp a target and practice grip.

To allow this freedom, it is essential that the tool that connects the human to the robot has specific characteristics. Since the features that must have the handle are too specific to be already on the market, a custom handle has been modelled, engineered, and then printed by a 3D printer. The first key feature is maintaining freedom in grip, without the risk of losing the handle during the movements. The second feature is the neutrality of the handle, which allows to use the same configuration for both upper limbs. Thus, is avoided the work for changing the configuration.

In principle, from several sketches (Figure 2.7), made on paper, the different handle types have been developed.

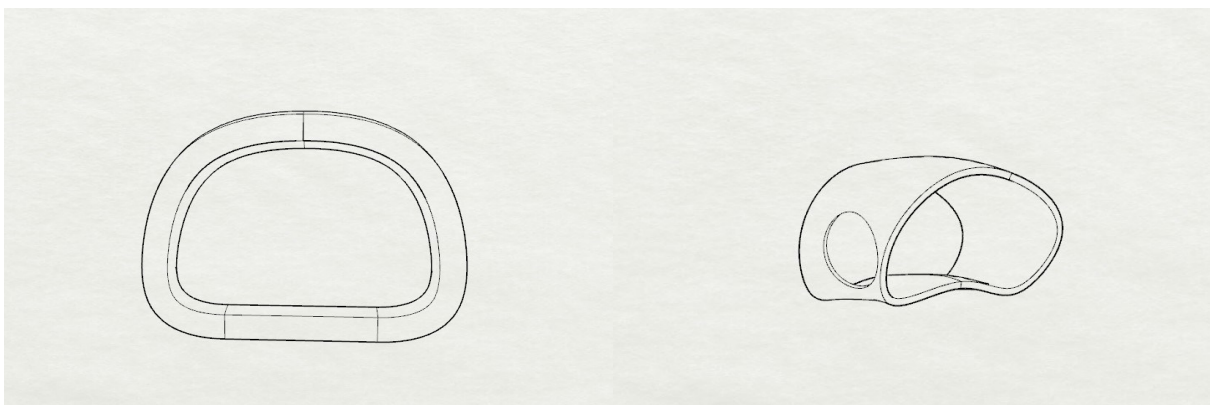


Figure 2.7.: Custom handle sketches.

The successive step has been the modelling of the custom handle by means of Rhinoceros 6, a commercial application software for 3D modelling of sculpted surfaces. Several trial models have been developed on Rhinoceros, all of which developed with new features, in addition to the key features, appreciable from Figure 2.8.



Figure 2.8.: Custom handle prototypes in rhinoceros.

The 3D model that has been chosen is represented on Figure 2.9. It is chosen because it meets all the planned key characteristics. Even more, due to its thickness, it increases the subject's confidence during the exercise.



Figure 2.9.: The custom handle that has been chosen.

Another key point in the modelling of the custom handle, has been the lock-in system. The idea was to produce a universal lock-in system, to allow an easy exchange from a tool to another, without the use of screws or complex lock systems. As it is possible to see from the Figure 2.9., there is a semi conical process on the top of the handle, which allow to insert the handle in a custom-made lock system. Accordingly, allowing an easy lock of the handle, leaving the custom part attached to the Tool Flange of the robot (Fig.2.10.).

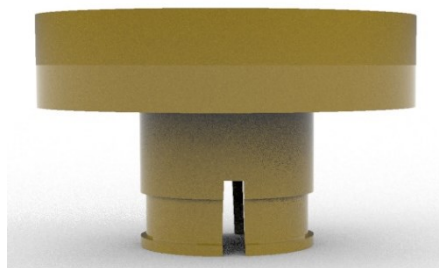


Figure 2.10.: Custom lock system.

The successive steps have been the engineering of the handle, analysing the dimensions of each component, based on the dimensions with respect the 50th percentile of the man hand (9.3 cm) [62], the rigidity of the material and the resistance of it. The last prototype was represented on different perspective views in all its components (Fig.2.11.).

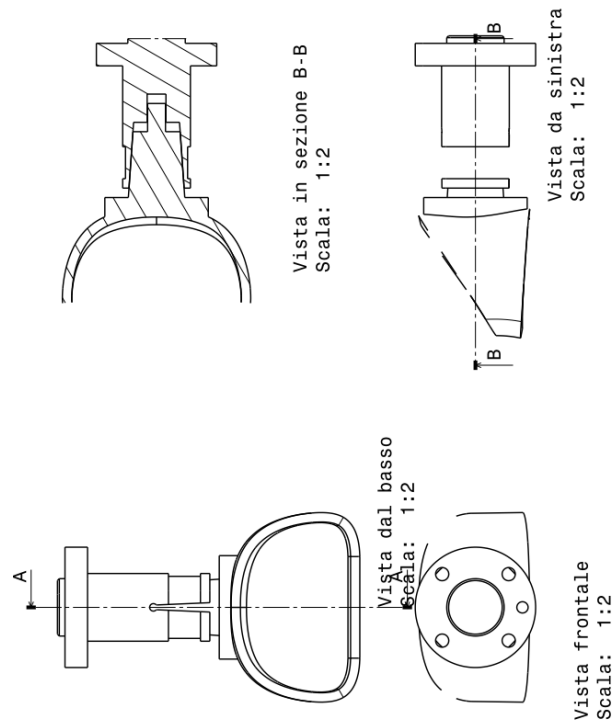


Figure 2.11.: Perspective views of the custom handle.

The last step has been the printing of the custom prototype using the Form 3+ 3D printer. The Form 3+ (Figure 2.12.) is a 3D printer based on the technology of Low Force Stereolithography (LFS), that basically uses linear illumination lased and a flexible tank, to turn liquid resin into flawless prints (XY resolution of 25 microns).



Figure 2.12.: Form 3+ 3D printer.

The Figure 2.13 shows all the components that compose the custom handle. From left: The handle, where the hand goes in; the cushion that makes the handle comfortable and, with different sizes; three hook and loop strips, to secure the thumb and the cushion; a locking system that secure the handle with the flange; the custom-made lock system and the screws that connects the system with the robot tool flange.

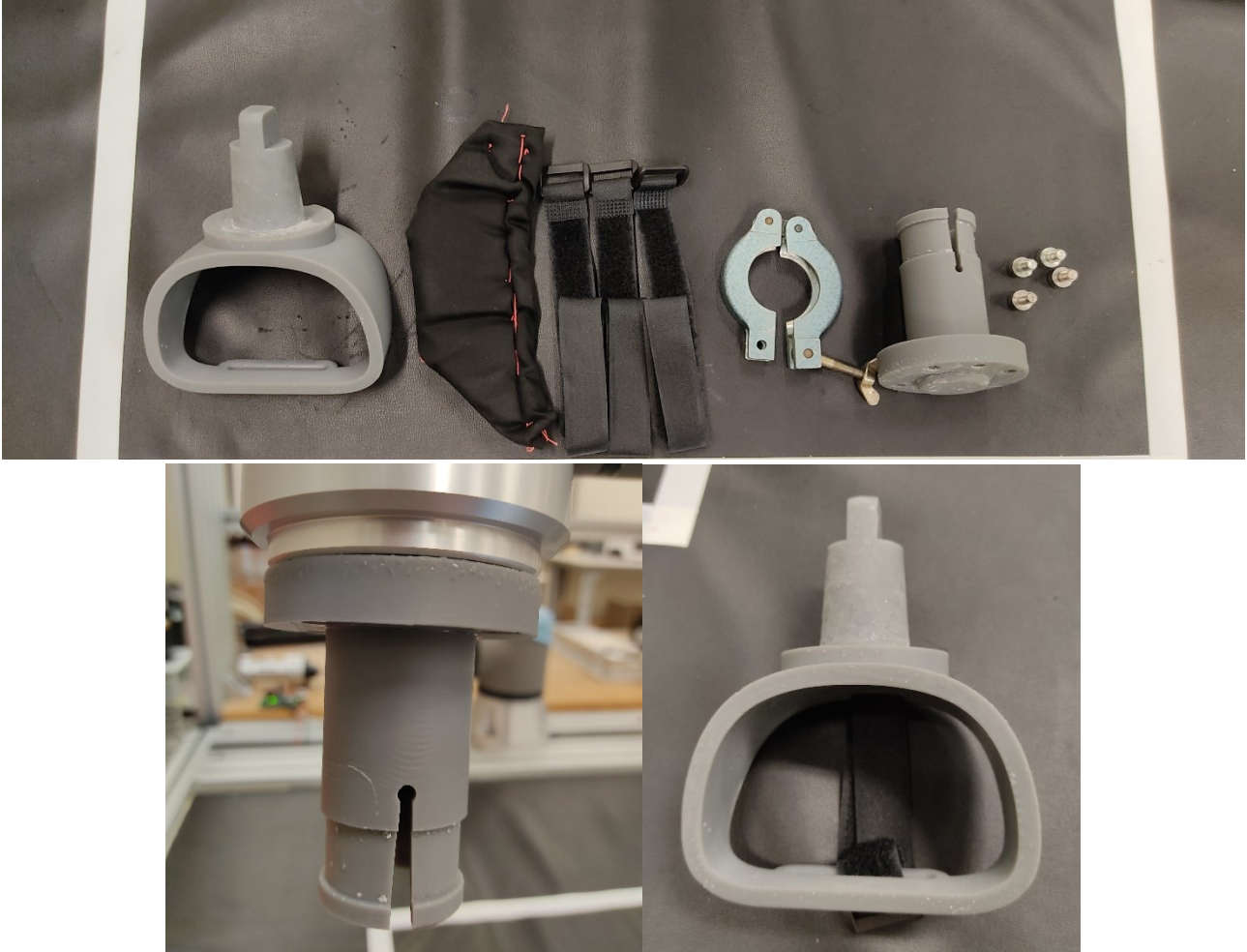


Figure 2.13.: The custom handle components.

Chapter 3.

Exercise development

The development of the rehabilitation exercise using UR5e cobot has followed different steps. The first step performed to build up the exercise framework has been the development of the fundamental force controls that act on it during the performance.

3.1. Control Laws

This study aims to develop a new exercise for neuromuscular rehabilitation of the upper limb, where, the background of this project is an experimental framework already tested, which has as limits the lack of freedom in the hand motion. Thus, the focus of this work is to allow a controlled free movement of translation along the X Y and Z axis and of rotation on the Z-axis, giving the possibility to grasp during the rehabilitation exercises.

3.1.1. Wrist Law

The first control law developed is a fundamental component of exercise. It is a force law assigned to the free movement of the human wrist during exercise. The principle at the base of the control equation is the development of an assisted movement that acts only of the 6th joint “Wrist 3” of the UR5e.

The development of the torque law applied on the 6th joint has been conceptualized as an active freedrive. Freedrive mode, in robotics, is defined as the state in which the robot can be moved by the operator without giving any force in opposition, keeping only the gravity compensation forces active, to maintain the configuration. More in detail acts on the torque generated along Z-axis in the TCP coordinates frame. Specifically, producing in input a torque generated by the hand along the Z axis, defined as Ch in this work, the robot gives in output a torque, named Cr , in the same direction with certain behaviour, assisting the human movement.

To find the control law that best fits the project goal, we first worked on the mathematical component.

The first step is to formulate an equation that has Ch as input and Cr as output components. For a given Ch , whether positive or negative, this equation must provide a Cr value that is congruent with the goal of the work, a proportional aid for rotation. Of course, this equation must have preliminary features:

- It must be stable near zero.
- It must have the maximum Cr output at the 25% of Ch .
- It must be stable for high values of Ch .

To find the law that best fits these characteristics, we started with a piecewise function (Fig.3.1.), which is a function built from pieces of different functions over different intervals, where each feature is respected by a constrain of stability. From here, two laws have been developed, one based on many

cubic polynomial equations (appendix 1), that allow having a huge control of output, but it is very complex. The second law is based on the same principles, but it is a simplified version, containing only a cubic polynomial equation (appendix 1) (eq.3.1).

$$Cr = 3 \left(\frac{a}{b^2} \right) (Ch - c)^2 - 2 \left(\frac{a}{b^3} \right) (Ch - c)^3 \quad (3.1)$$

Equation 3.1. *cubic polynomial control law.*

After the first mathematical approach, the two laws have been implemented in the Simulation software Simulink, to perform the analysis of the stability. A simple model has been developed in Simulink (Fig.3.2). The model represents the implementation of the control law in a simple robot system constituted by a single rotational joint, where the dynamics are described by the expression 3.2 of a generic n-DOF manipulator.

$$B(q)\ddot{q} + C(q, \dot{q})\dot{q} + G(q) = \tau \quad (3.2)$$

Equation 3.2. *Manipulator dynamics equation.*

The $B(q) \in \mathbb{R}^{n \times n}$ is the inertia matrix, $C(q, \dot{q}) \in \mathbb{R}^{n \times n}$ is the Coriolis matrix and $G(q) \in \mathbb{R}^{n \times 1}$ is the gravitational force vector; q , \dot{q} and $\ddot{q} \in \mathbb{R}^{n \times 1}$ are respectively joints position, velocity and acceleration. The right-hand side of 2.2 is the input torque/force vector $\tau \in \mathbb{R}^{n \times 1}$.

The input of the Simulink system is a trajectory generated through multiple waypoints using trapezoidal velocity profiles. The output is represented by the displacement, velocity and acceleration of the robot during the trajectory, controlled by the customs law.

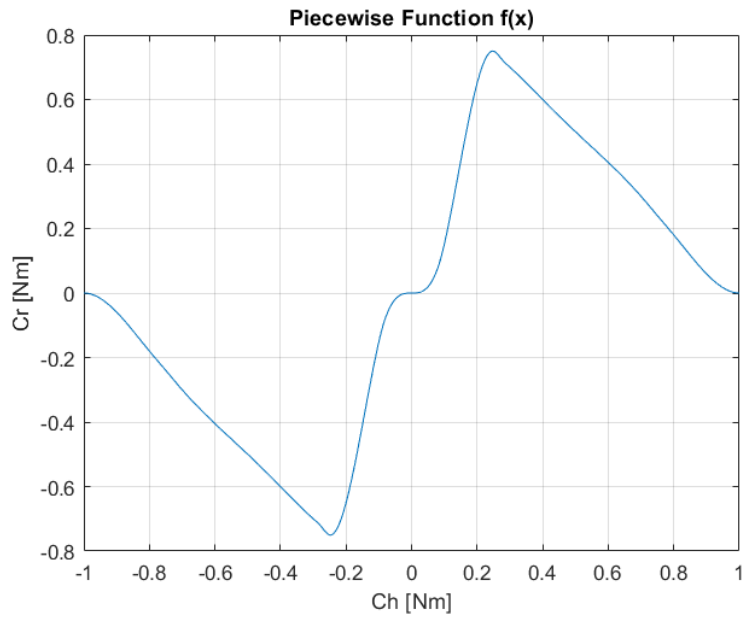


Figure 3.1.: Representation of the control law.

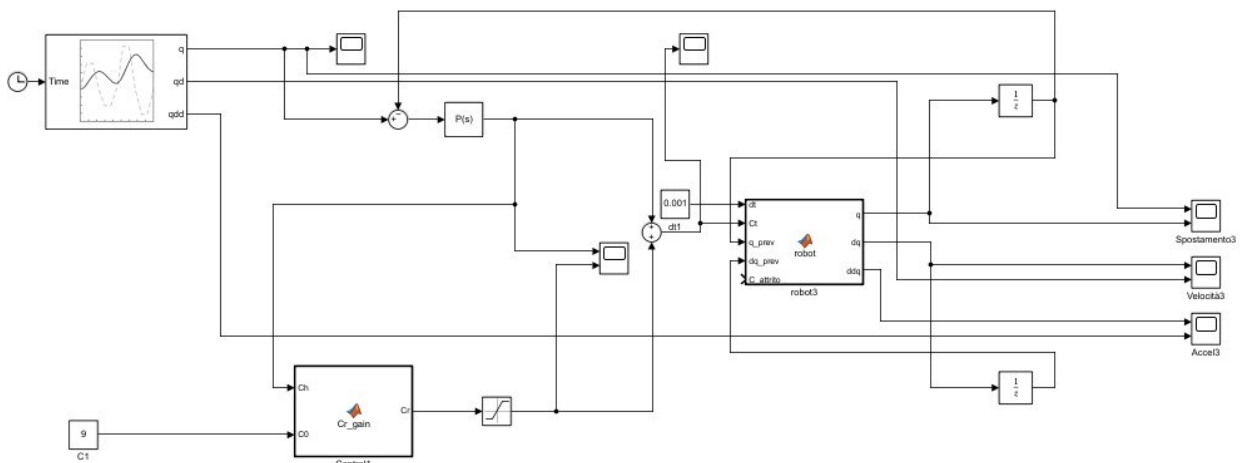


Figure 3.2.: Simulink model.

The last step has been the integration of the two laws in the UR5e robot. A simple program has been written in URScript, in which the robot enters in force mode with only a DOF with respect to the rotation along Z-axis of the TCP. To analyse the performances of the two control laws on the 6th joint, the data were acquired, and the best law was chosen.

3.1.2. Impedance Control Law

To move the kinematic closed chain formed by the human upper limb and the robotic arm along a planned trajectory to reach a target, the robot must have several safety systems, that can be already integrated or can be applied through an external control generated by law. A crucial control that has to be implemented to perform rehabilitation exercises, is the Impedance control.

The impedance control is a dynamic control related to force and position, always used in the HRI environment. In detail, impedance control regulates the relationship between force and position on one side and velocity and acceleration on the other side. The desired performance is specified through a generalized dynamic impedance, based on complete mass-spring-damper equations (eq. 3.2).

On these principles, ad hoc impedance control has been developed. Based on a spring-like behaviour, this control regulates the relationship between the input pose of the TCP with respect to the planned trajectory and the output forces and torques generated by the robot to maintain that trajectory.

The spring-like equation at the base of this control is:

$$k = \frac{(-k_f r^2)}{r_0^3(2r-3r_0)} \quad (3.3)$$

Equation 3.3. Spring-like equation.

K_f is the parameter representing the stiffness of the spring. Through this parameter, the robot generates a force opposite to the direction if the latter does not respect the defined trajectory.

The parameter r is the radius that delimits the stiffness of the spring, r_0 express the initial radius.

It is important to mention the fact that this impedance control, works to maintain the planned trajectory generated by the robot, analysing the TCP pose in relationship with the target pose.

The output of this control gives back the counter force along the three axes $x y z$ of the TCP coordinate frame, to avoid undesired movements.

3.1.3. Robot Force

The latest force law applied on the UR5e to perform the rehabilitation exercise is based on the concept of assistive mode and resistive mode. It has been implemented a law in which the robot generates a force, depending on the human force acquired during the process. The output force acts along the line generated by the planned trajectory between TCP and target, and the direction of the force depends on the exercise modality.

3.2. Rehabilitation Exercise

The exercise framework used to perform the rehabilitation of the upper limb has the main aim to restore of proprioceptive abilities, helping the subject to perform repetitive movements following a precise path in the workspace, and restore the muscular activity involved during the movement.

It is based on the principle of HRI rehabilitation, using UR5e connected at the End-Effector with the subject hand, forming a kinematic closed chain made up of the robot and the human arm.

The Figure 3.3. depicts the scenario of the exercise, constituted by the subject and the UR5e.

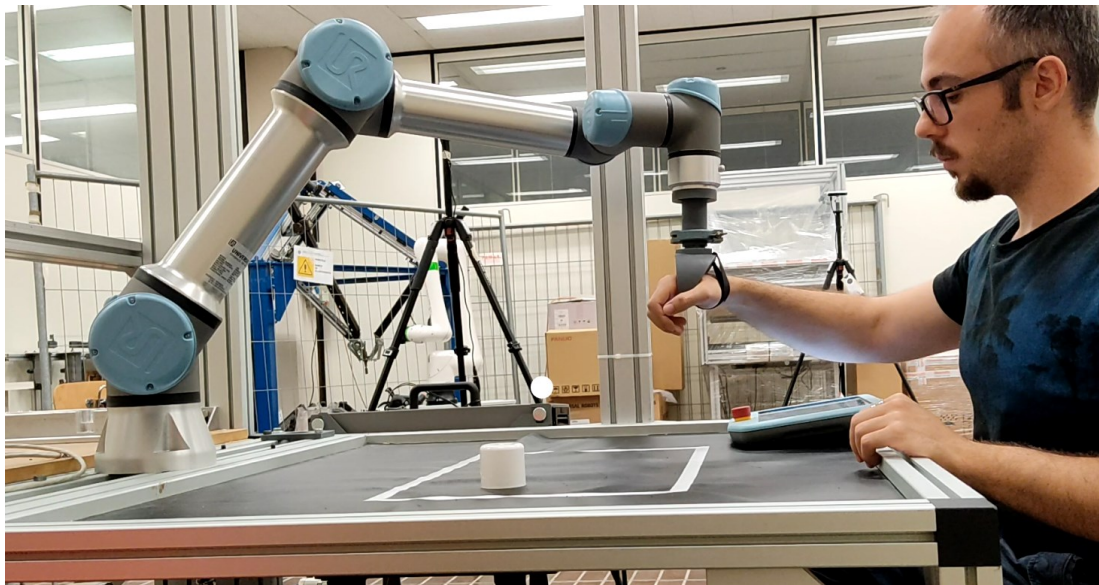


Figure 3.3.: Exercise configuration.

At principle, the UR5e has to be powered on, and the exercise has to be loaded in the software.

The subject connects his hand with the cobot and the supervisor runs the program. The exercise is designed to have full flexibility, so, at the beginning the supervisor will measure the anthropometric parameter based on the distance between the centre of his hand and the middle phalanx of the middle finger of the subject, to set the translated TCP.

Immediately after, the supervisor chooses the arm that will go under rehabilitation based on the subject's case history, and depending on which one is to undergo therapy, the robot will position itself in the operating space in a position congruent with the case. The fixed positions in which the robot moves in these stages are planned on the code, setting the pose of the TCP in the space in such a way as to increase the ergonomics of the hold.

The next step is the calibration of forces. The first is the force generated by the relaxed patient's arm, while the second is the force imparted by the patient. Both quantities are analysed by the robot and used during exercise in the form of resistant force.

Then, the subject can choose the mode of exercise from three options:

- Easy mode: the robot gives back to the subject a force proportional to the one calibrated that helps the subject to follow the planned trajectory. The robot is in assistive mode.
- Medium mode: the robot doesn't help the subject at all. In this case the force explained in the section 3.1.3. is set to zero. The subject has to move from the start all over the trajectory by himself.
- Hard mode: the robot gives back a force proportional to the one calibrated, but in the opposite direction with respect the one generated by the subject. The robot work in resistive mode.

In every modality there are two controls that are always active, the impedance control and the wrist law, that allow a certain mobility.

In each case, the subject can choose the number of repetitions of execution and the position of the target, inside the working space.

All the area delimited by a white line, in Figure 3.4, constitutes the working table. All this area is controlled in real time by the Cognex 2D camera (Fig. 2.6). The task that fulfils the camera during the exercise is to analyse the position of the target, in the workspace and extract the coordinates, in this way the robot plans the trajectory of the exercise which, has as its starting point the position of the TCP at the beginning of the exercise and, as the end point the position of the target acquired by the camera.

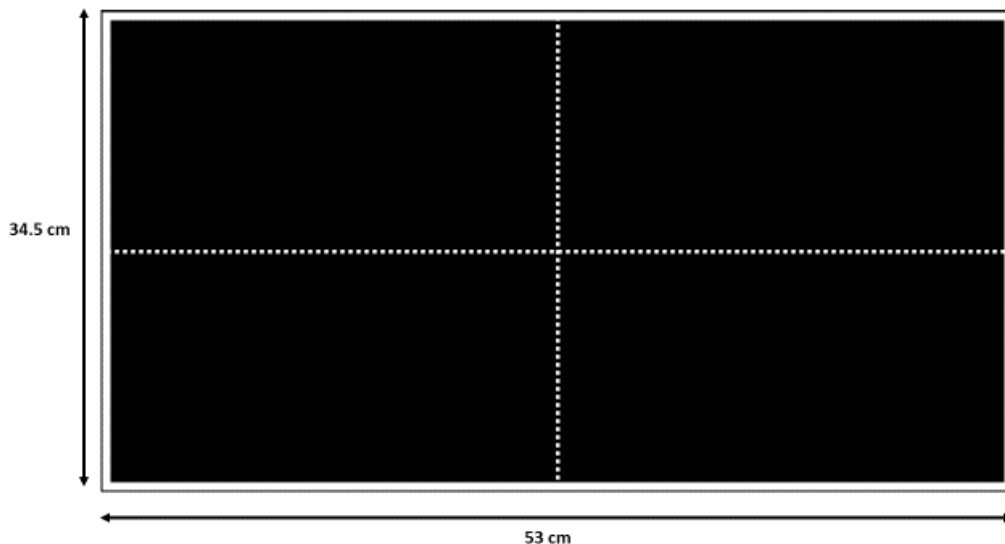


Figure 3.4.: Working table.

At the end of the exercise the subject can choose to restart the whole process in a different difficulty or can move to the other arm.

3.3. Data Acquisition

The data has been acquired using the URLog viewer, software that allows to record data during the robot performances and can display them in real-time. Ten healthy volunteers have been recorded during the exercise, 8 male and 2 female (mean age of 30). Each subject has been instructed on all the steps of the exercise and has been supervised during the duration of it. During all the exercises, data were recorded on the PC.

The exercise protocol is based on:

- 5 repetitions in easy mode with right arm.
- 5 repetitions in medium mode with right arm.
- 5 repetitions in hard mode with right arm.
- 5 repetitions in easy mode with left arm.
- 5 repetitions in medium mode with left arm.
- 5 repetitions in hard mode with left arm.

In each mode the target is moved in a fixed position on the working plane, this procedure is the same for each subject, Figure 3.5 represents the positions on the table in each exercise.

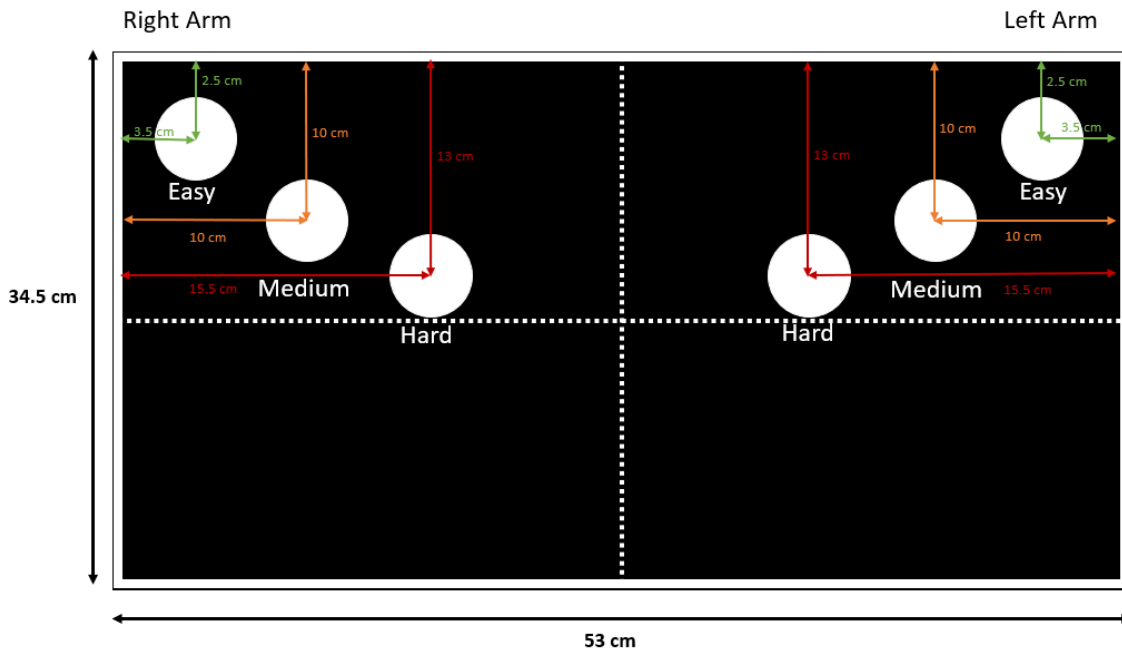


Figure 3.5.: Target positions during the exercise.

3.4. Data Processing

The data acquired during the recording sessions were stored in .csv files on the personal computer. The processing part of the data was performed using Matlab in each of its steps.

First, all .csv files containing data for each subject in the different exercise modes were probed, to assess the quality of the recording.

Next, the data were filtered by type, taking into consideration only those records useful for the analysis process. So, data like “actual TCP force” and “actual TCP pose” were taken into consideration. After that, the data were windowed into different segments, depending on the range of time in which the subject performed each repetition of the exercise.

Having all the data prepared for the analysis, the next step was the extraction of features relevant to our goal, divided into three fields:

- Trajectory features: the error between the TCP poses actual trajectory and the planned one has been analysed, studying the mean, the maximum and minimum value.
- Force features: the mean force, minimum and median force have been evaluated.
- Statistics features: in each subject, the correlation factor between the TCP pose and the force has been analysed.

One of the trajectory features analysed on results is the Fréchet distance. The Fréchet distance is a measure of similarity between two curves, P and Q. It is defined as the minimum cord-length sufficient to join a point traveling forward along P and one traveling forward along Q, although the rate of travel for either point may not necessarily be uniform.

These data were extracted for the individual subject and the entire data sample, allowing the investigation of a possible statistical significance.

Chapter 4.

Results

This chapter will present the results of the experiments. These are divided into two sections:

- First, there is a description of the results given by the choice of control law on the 6th joint of the UR5e.
- The second section contains the results of the rehabilitation exercise, based on the analysis of data acquired from 10 healthy subjects. The analysis is focused on the difference between the planned trajectory and the real one, and on the forces applied during the performance.

4.1. Results from the control law

The two control laws presented in the paragraph 3.1.1. of the chapter 3, developed to produce a robot torque in output to help the rotation along the Z axis of the TCP, have been tested, to decide which one works better for the purpose of the rehabilitation exercise.

Figure 4.1. shows the difference between the two specific control law, named as “cubic” and “piecewise”, the names are based on their characteristics, compared with the freedrive mode, a mode of the robot in which the joints can move freely without receiving internal help from the robot itself. The representation in the figure is based on data acquired during a session of 60 seconds, in which the human can only perform the rotation of the 6th joint around the Z axis of TCP frame.

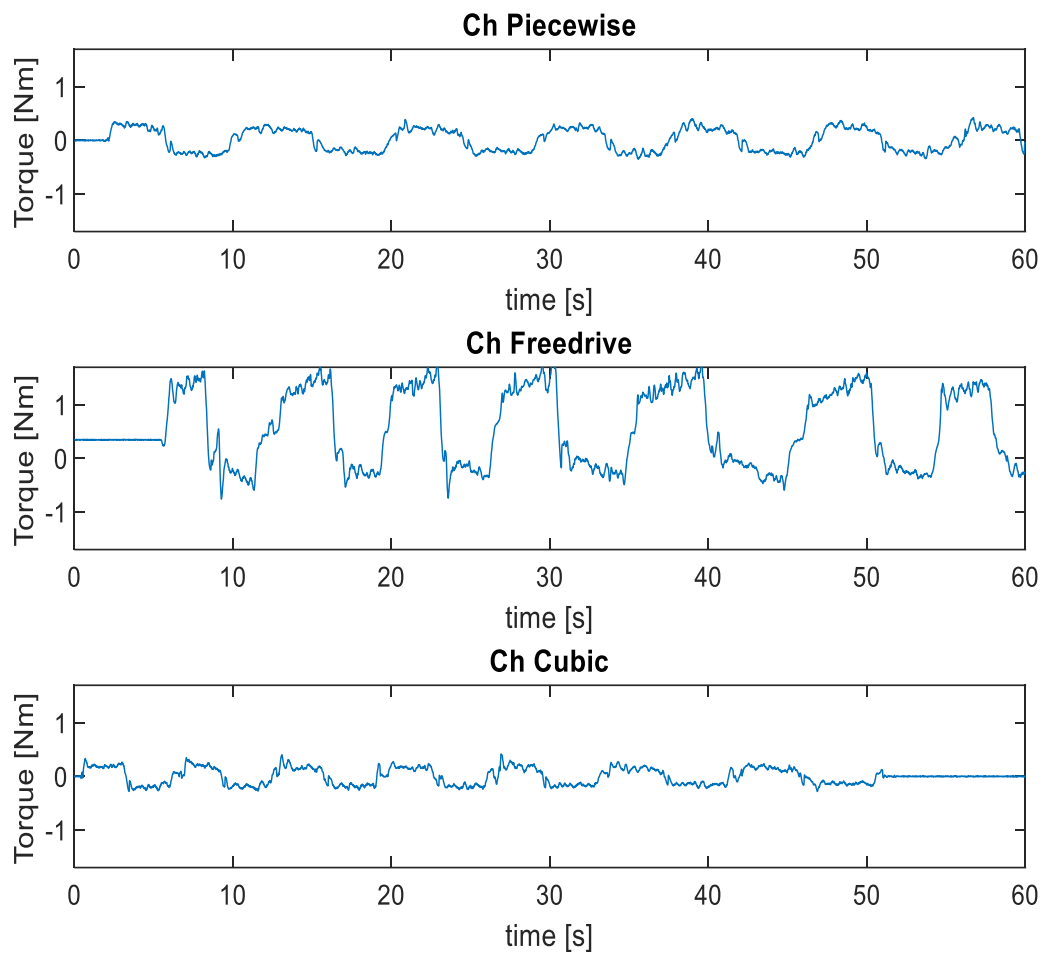


Figure 4.1.: Comparison between the control laws and the freedrive mode.

From Figure 4.2. it can be appreciated a stability test performed on the three different modes, respectively with piecewise law (Control 1), freedrive mode (Control 2), and cubic law (Control 3). In this case the acquisition of data is based on a 60 second session in which the robot has no interaction with the human.

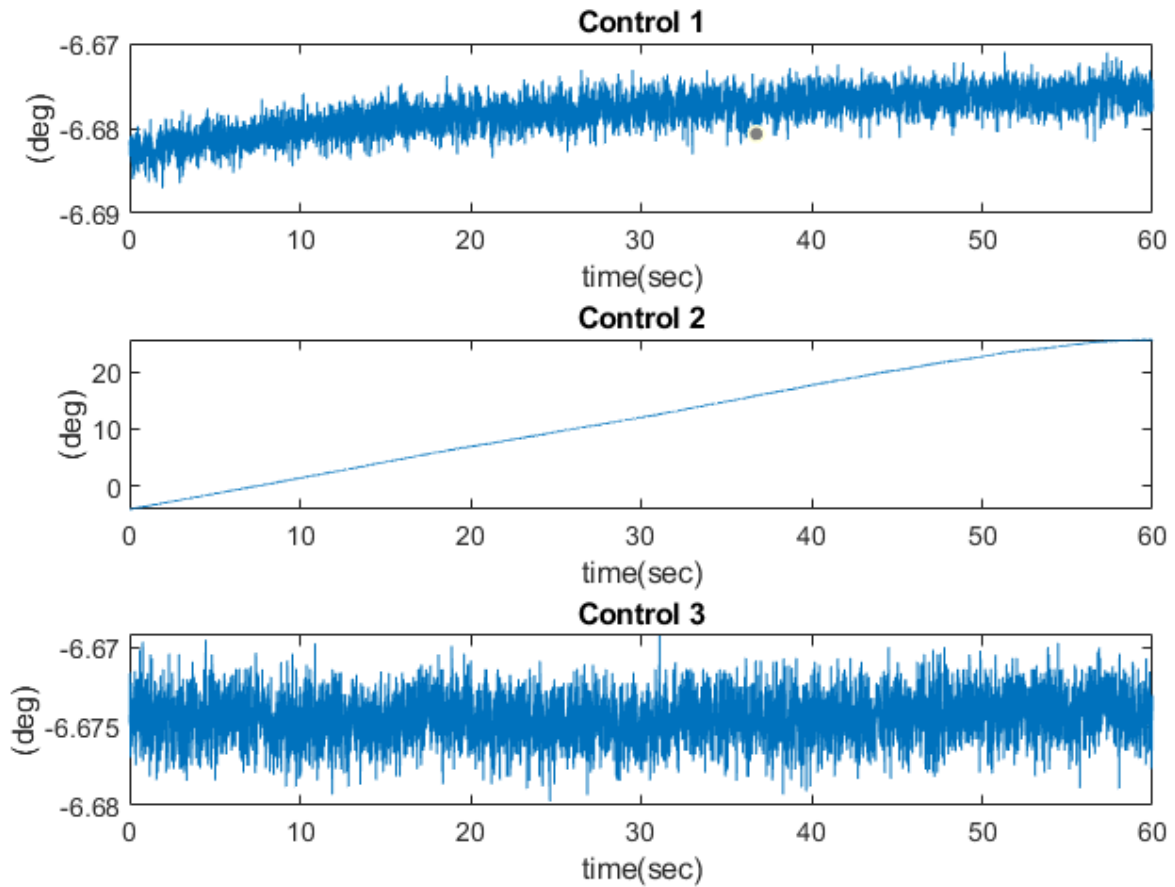


Figure 4.2.: Comparison between the control laws and the freedrive mode with no inputs.

Then, the torque generated by the two control laws has been compared to the angle of rotation, in the recording session based on a rotation of 90° in the clockwise and counterclockwise directions. The results are shown in Figure 4.3.

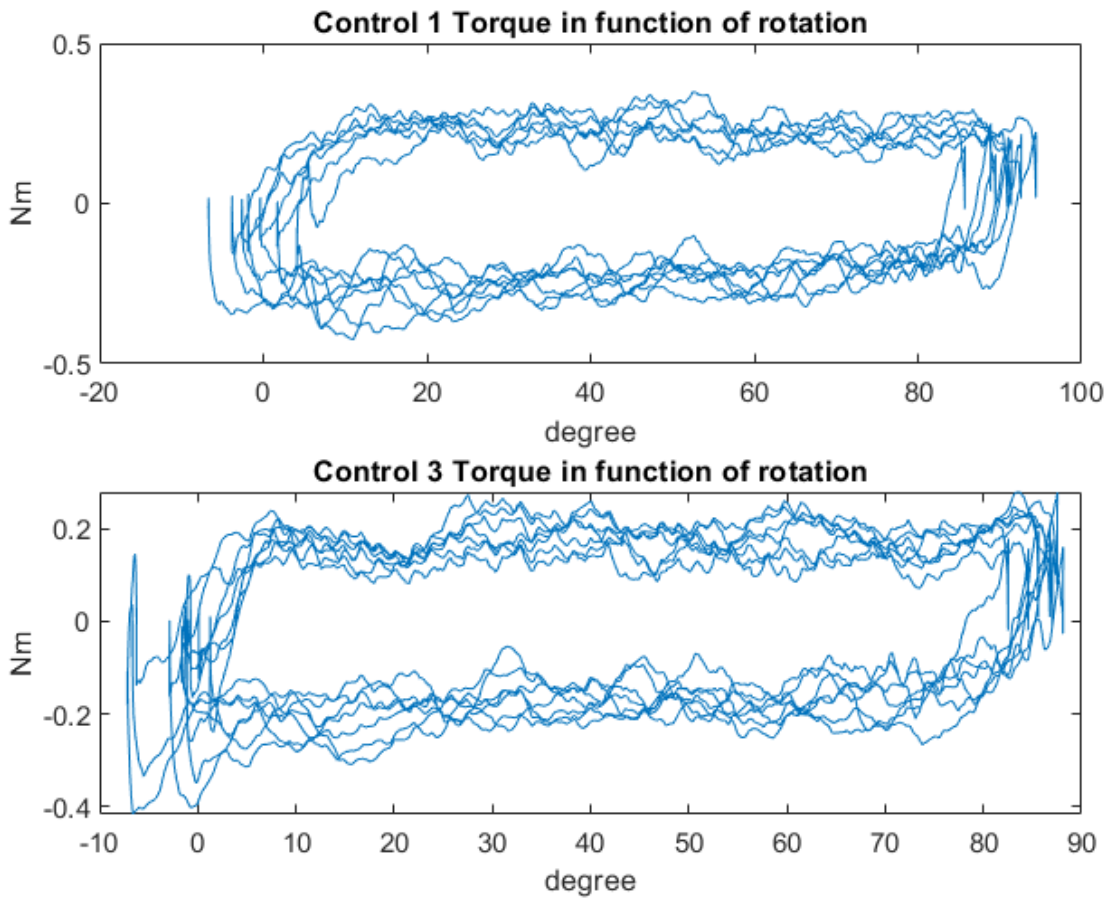


Figure 4.3.: Control law relationship with the angle of rotation.

Results from data acquisition on the comparison between controls are listed in Table 4.1. as follows.

Table 4.1.: Results from the comparison of the two control laws and freedrive mode.

	Piecewise law	Cubic law	Freedrive
Max Torque [Nm]	0.4234	0.4168	1.6708
Mean Torque [Nm]	0.20	0.1296	0.7062

Analysing the results proposed by the various experiments, based on the values of the average torque imparted by humans during the exercise, on the stability of the control without external inputs (Fig. 4.2.) and on the complexity of the law itself, the control chosen was the one defined as the cubic law, expressed in Equation 3.1. present in Chapter 3.

4.2. Results from the rehabilitation exercise

The results found from the data acquired during rehabilitative exercise for the upper limb are presented as follows. They are divided into two sections: trajectory analysis and, force analysis.

4.2.1. Trajectory results

The trajectory generated by the subject's hand during the exercise to reach the target is calculated based on the coordinates given by the variation of the robot's TCP pose during the performance. All the trajectories generated during the exercise with the right and left arm in easy, medium, and hard modes, respectively, are represented below, from Figure 4.4.a) to Figure 4.12.a). Next to the human-generated trajectories are represented the trajectories planned by the robot by calculating the distance between the starting point and the endpoint (target position) (Fig 4.4.b-12. b).

Figure 4.13. (a, b, c) represents the actual TCP trajectories of the right arm of Subject 0 during 5 repetitions in easy mode, medium mode, and hard mode. Furthermore, the actual TCP trajectories of the right arm of Subject 0 during 1 repetition in easy mode, medium mode and hard mode are represented in Figure 4.14. (a, b, c).

Easy Mode:

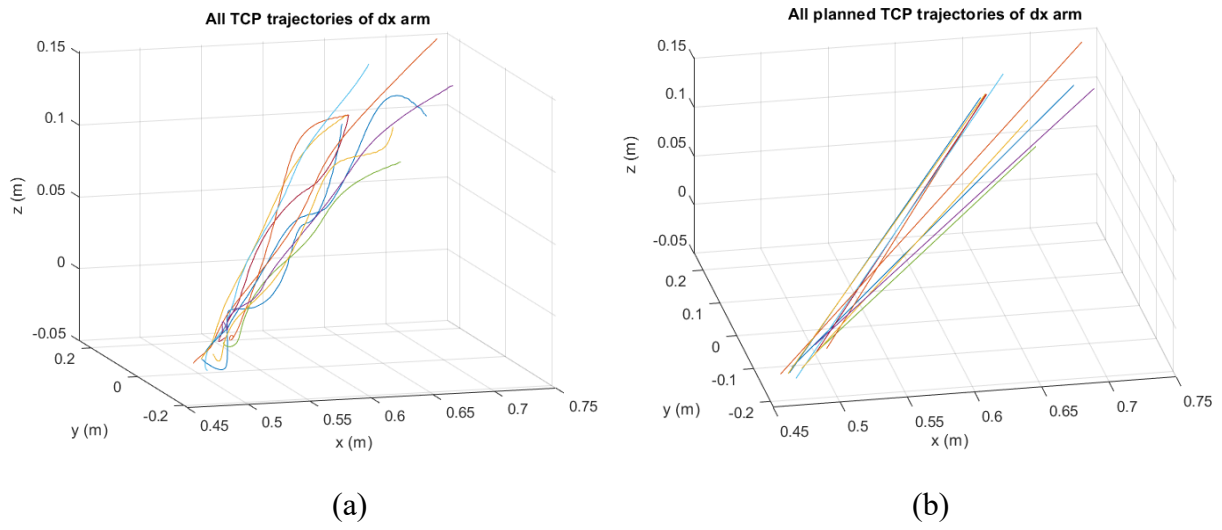


Figure 4.4.: Easy mode. **a)** All actual TCP trajectories of right arm. **b)** All planned TCP trajectories of right arm.

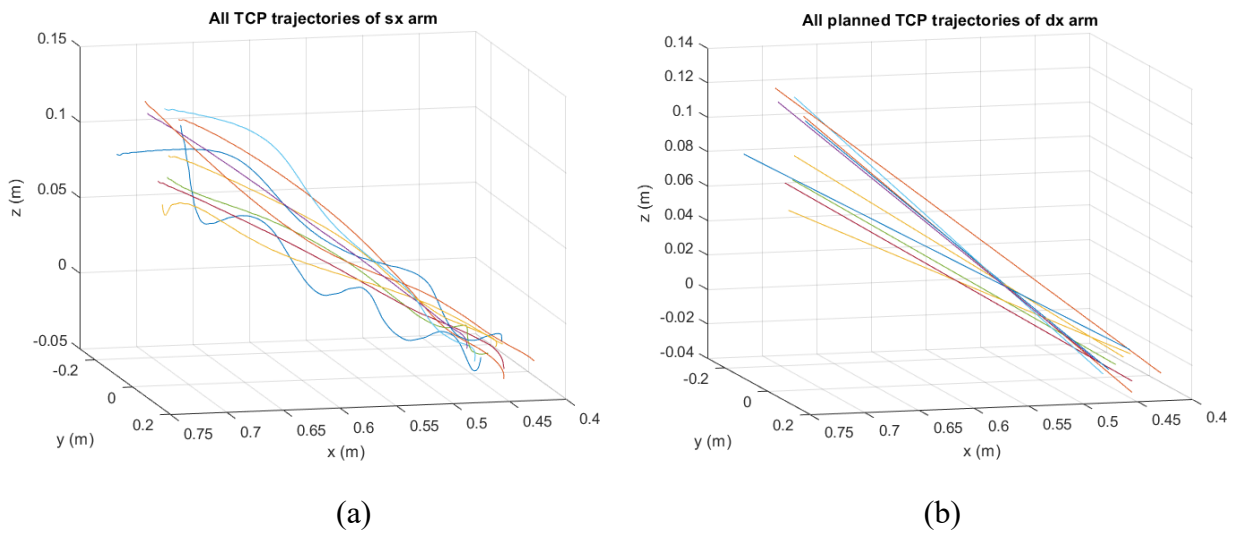


Figure 4.5.: Easy mode. **a)** All actual TCP trajectories of left arm. **b)** All planned TCP trajectories of left arm.

Medium Mode:

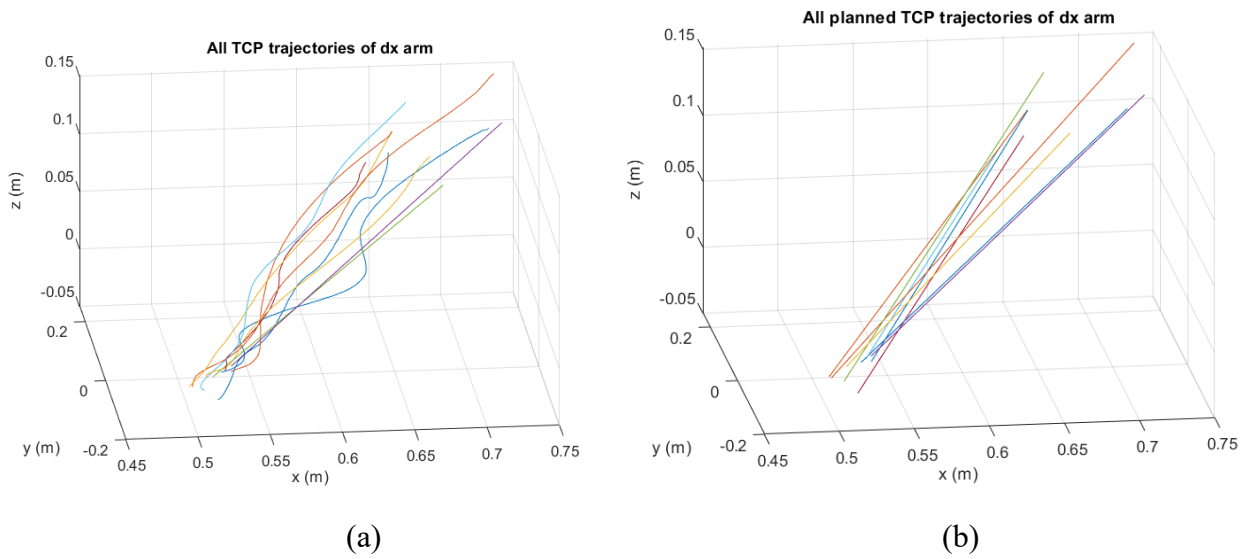


Figure 4.6.: Medium mode. **a)** All actual TCP trajectories of right arm. **b)** All planned TCP trajectories of right arm.

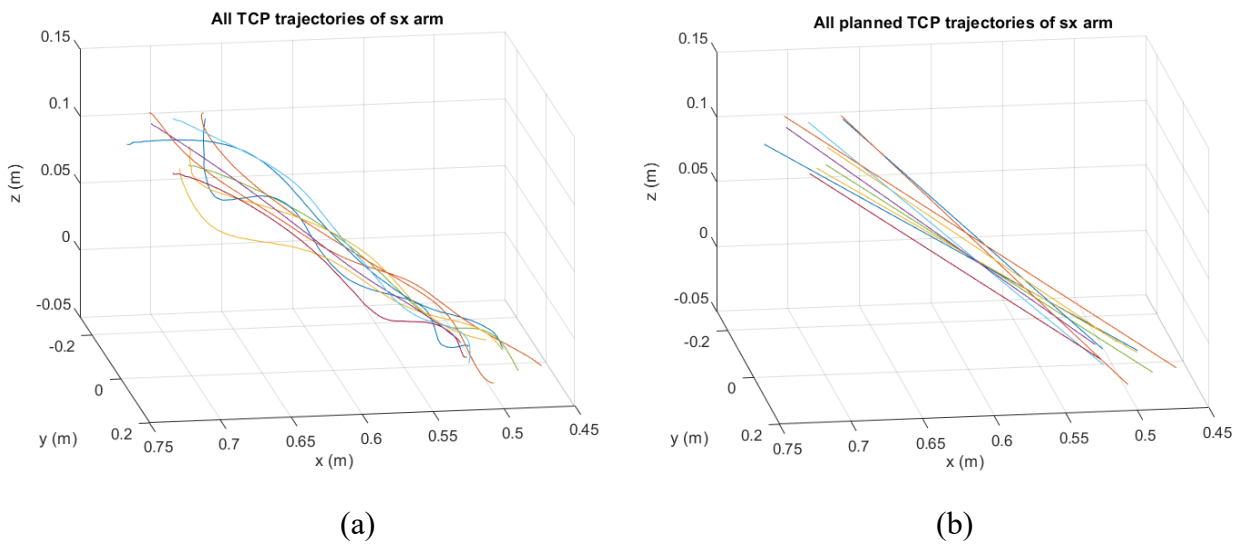


Figure 4.7.: Medium mode. **a)** All actual TCP trajectories of left arm. **b)** All planned TCP trajectories of left arm.

Hard Mode:

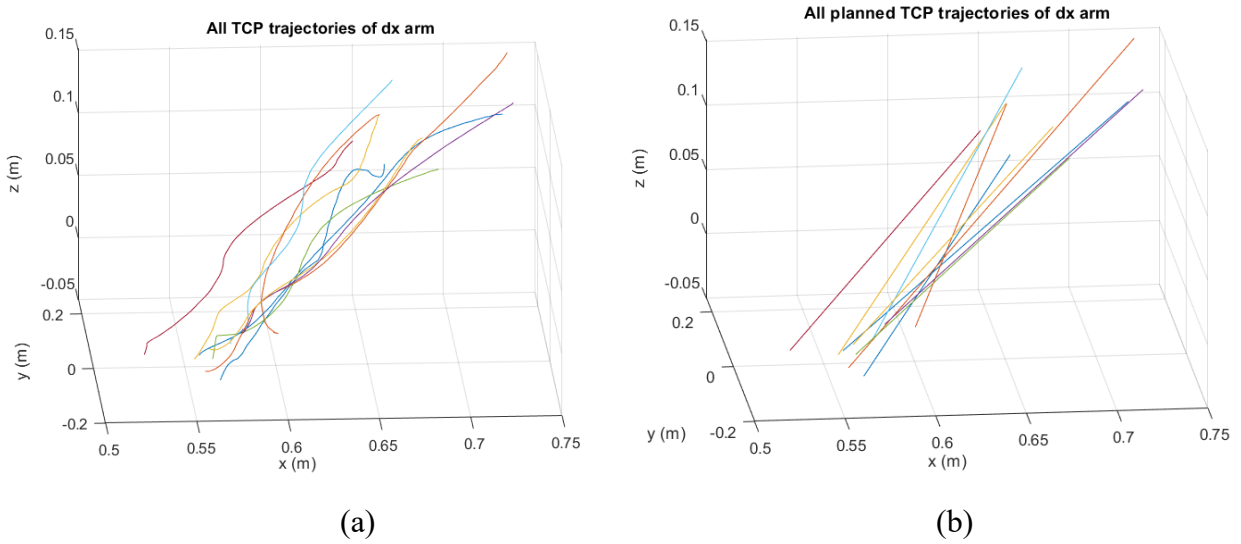


Figure 4.8.: Hard mode. **a)** All actual TCP trajectories of left arm. **b)** All planned TCP trajectories of left arm.

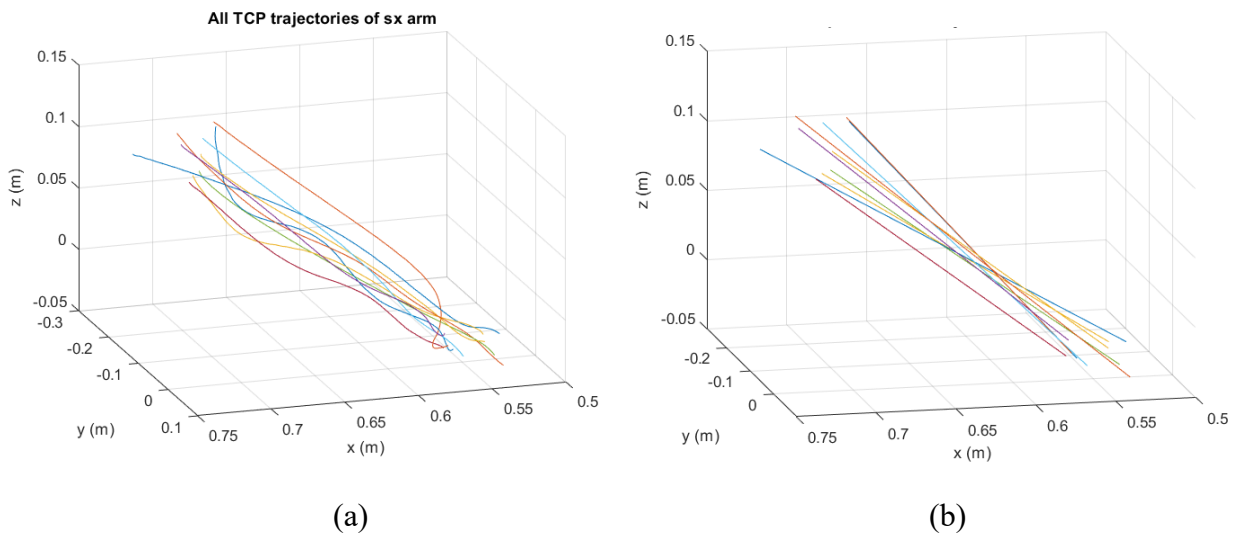
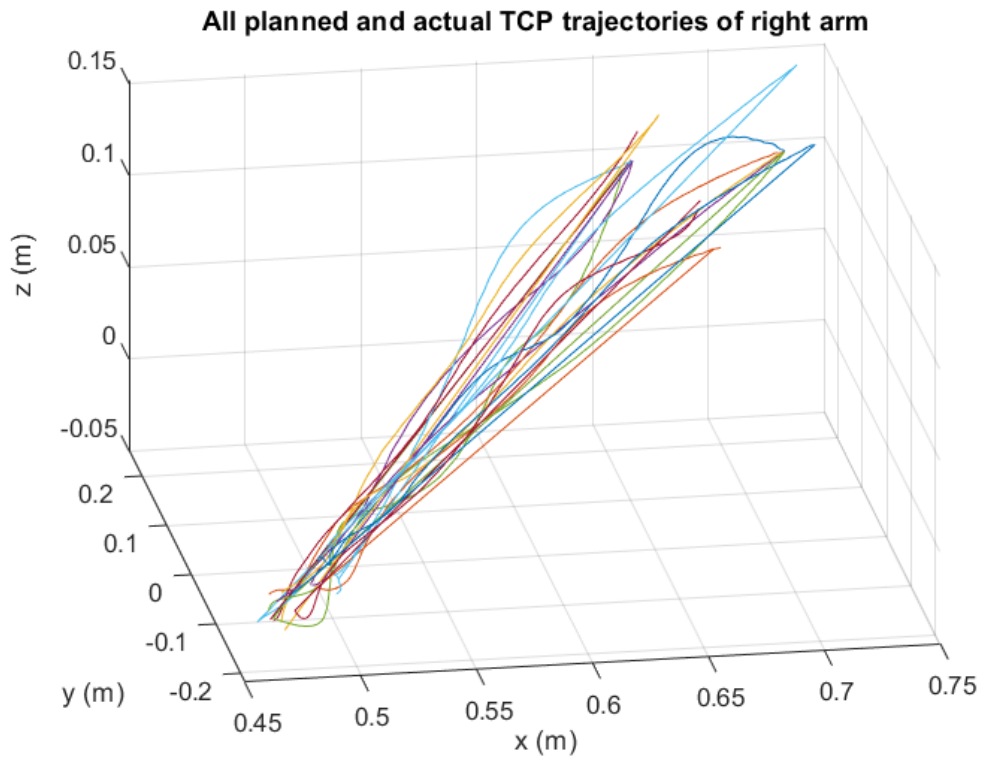
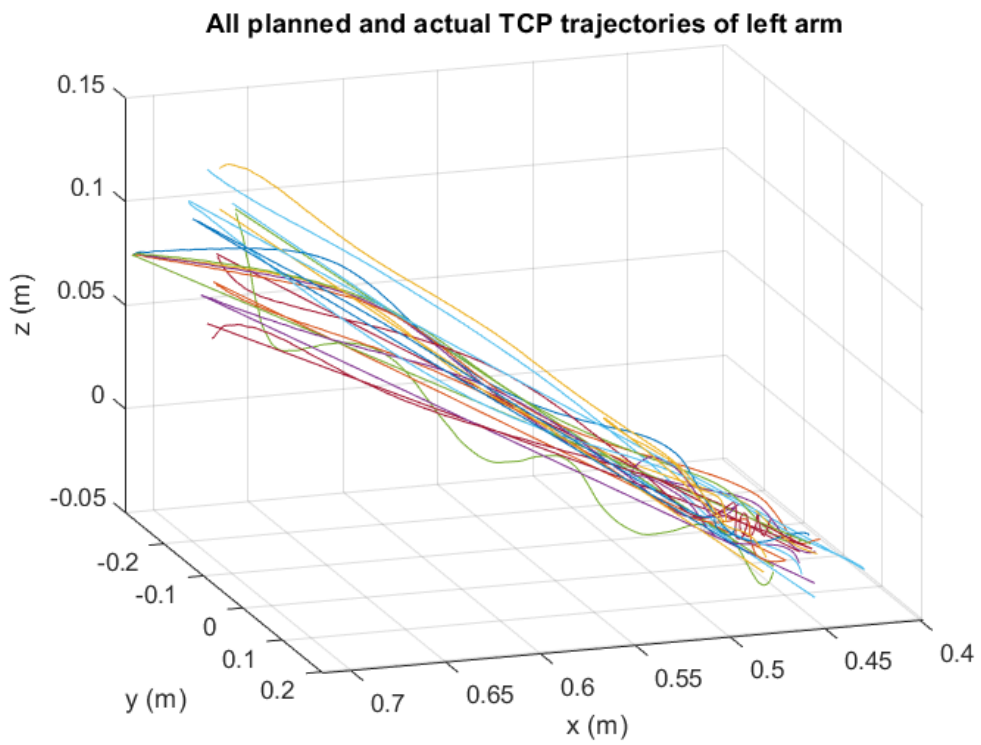


Figure 4.9.: Hard mode. **a)** All actual TCP trajectories of left arm. **b)** All planned TCP trajectories of left arm.

Easy Mode:



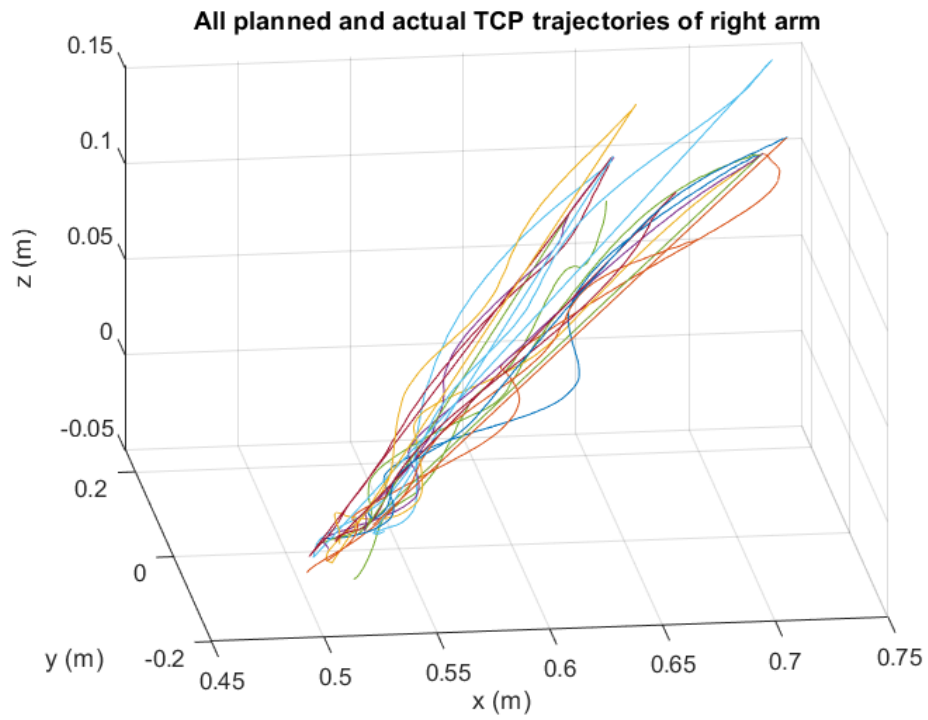
(a)



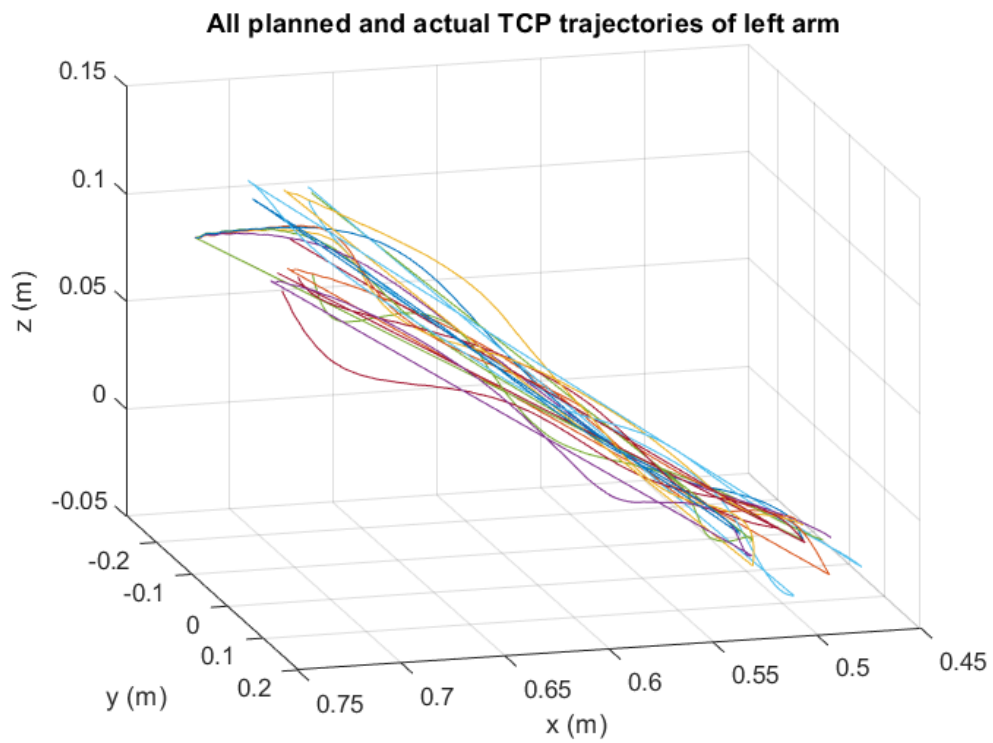
(b)

Figure 4.10.: Easy mode. **a)** All planned and actual TCP trajectories of left arm. **b)** All planned and actual TCP trajectories of left arm.

Medium Mode:



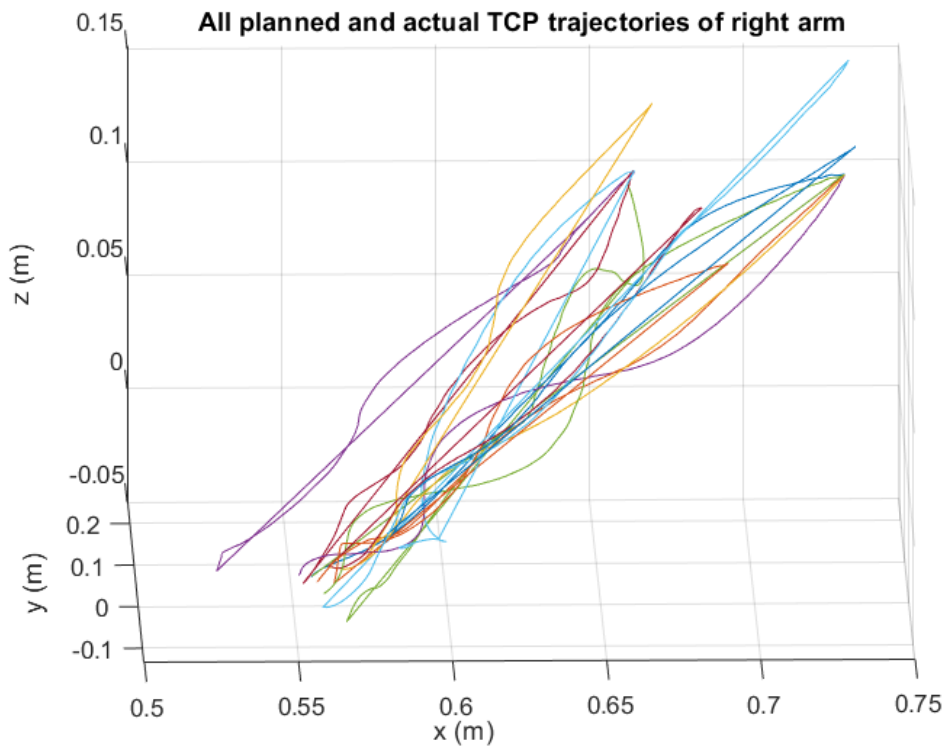
(a)



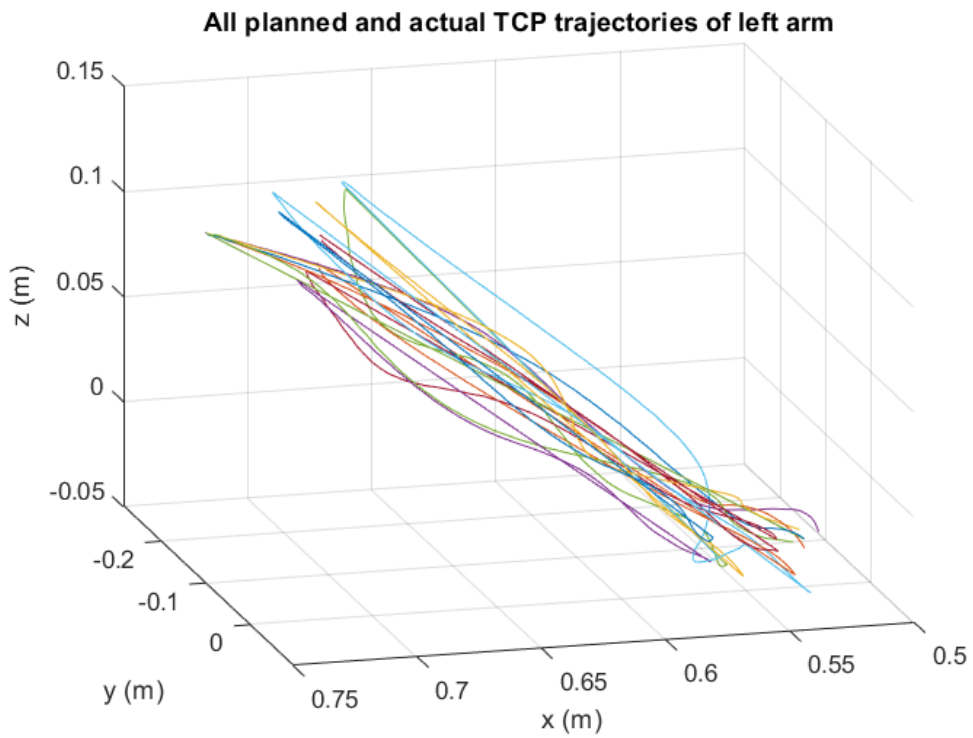
(b)

Figure 4.11.: Medium mode. **a)** All planned and actual TCP trajectories of left arm. **b)** All planned and actual TCP trajectories of left arm.

Hard Mode:



(a)



(b)

Figure 4.12.: Hard mode. **a)** All planned and actual TCP trajectories of left arm. **b)** All planned and actual TCP trajectories of left arm.

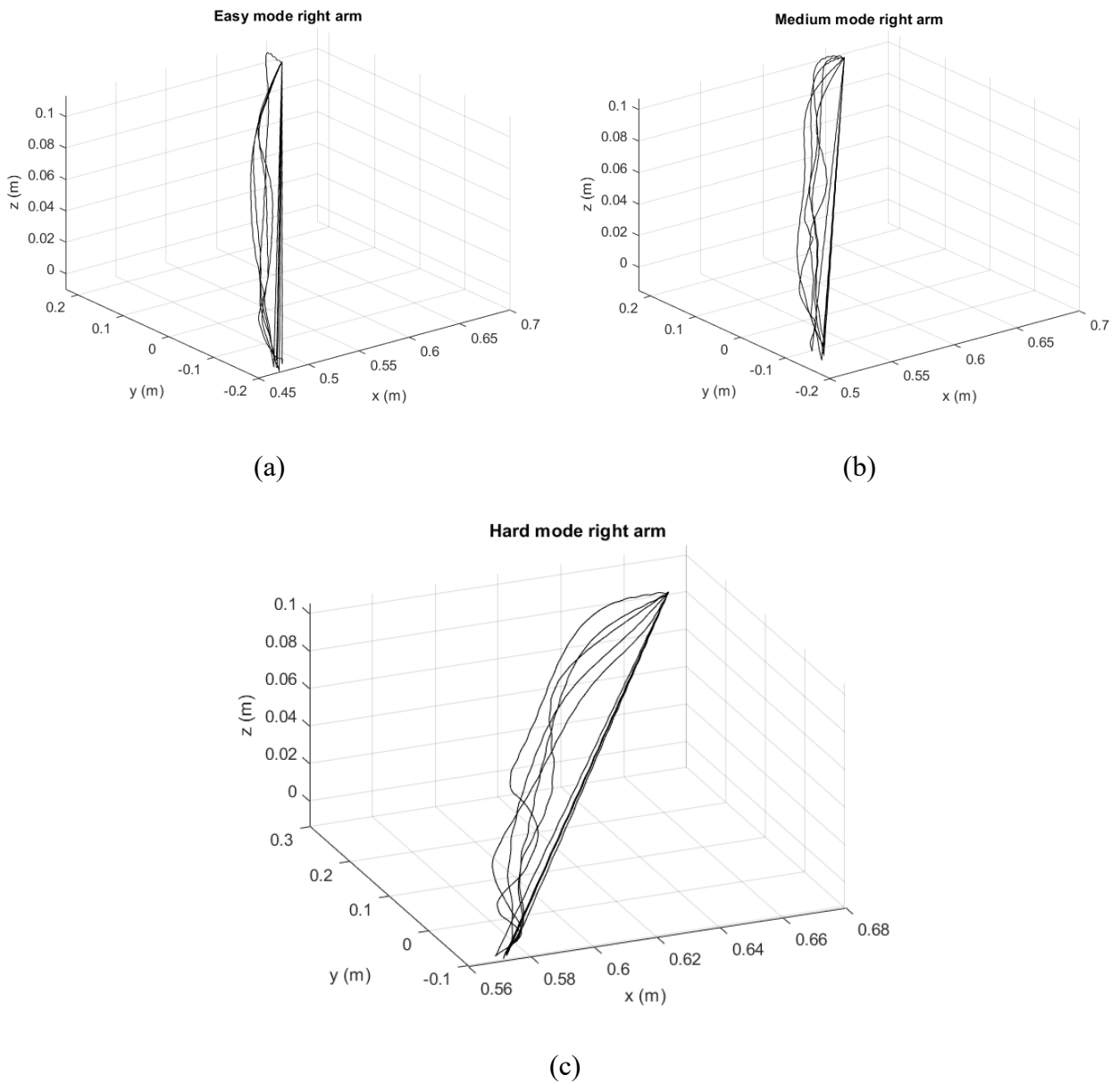
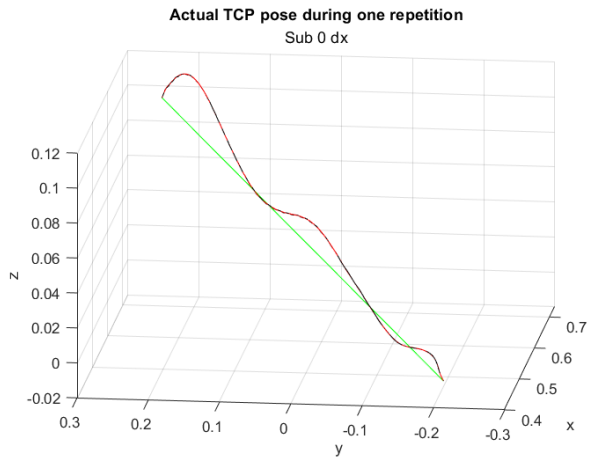
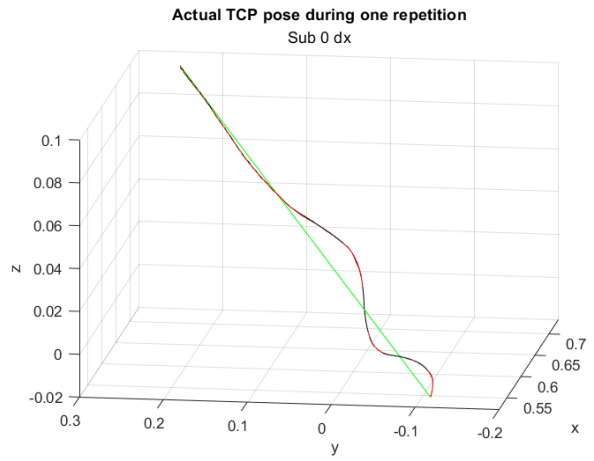


Figure 4.13.: Right arm trajectories of Subject 0.

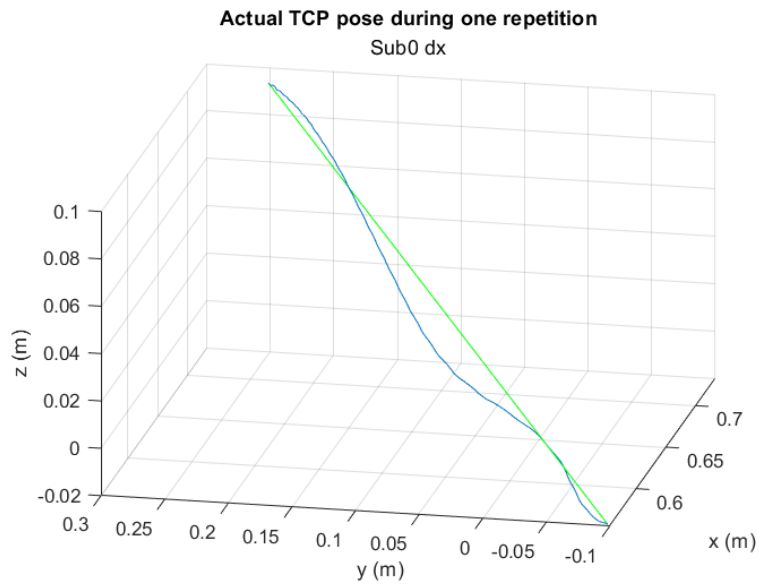
a) Actual TCP trajectories of right arm during 5 repetitions in easy mode. **b)** Actual TCP trajectories of right arm during 5 repetitions in medium mode. **c)** Actual TCP trajectories of right arm during 5 repetitions in hard mode.



(a)



(b)



(c)

Figure 4.14.: Right arm trajectories Subject 0.

a) Actual TCP trajectories of right arm during 1 repetition in easy mode. **b)** Actual TCP trajectories of right arm during 1 repetition in medium mode. **c)** Actual TCP trajectories of right arm during 1 repetition in hard mode.

The quantitative results from the trajectory analysis are listed in Table 4.1., Table 4.2. and Table 4.3., respectively for easy, medium, and hard mode.

From them, it is possible to appreciate the value of mean error, median error, maximum error, minimum error, and Root Mean Square Error (RMSE), in which the error represents the difference between the actual and the planned trajectory.

The last column of each table presents the Fréchet distance value, which represents the similarity between curves that consider the location and ordering of the points along the curves.

The Table 4.4. contains the mean error from all the subjects in different modalities.

Table 4.2.: Distance between the actual and planned trajectory for each subject in easy mode. R and L represents Right arm and Left arm. RMSE is the Root Mean Square Error.

Easy Mode		Mean error	Median error	Max error	Min error	RMSE	Fréchet distance
		(m)	(m)	(m)	(m)	(m)	(m)
Sub 0	R	0.0400	0.0360	0.0727	0.00010	0.0210	0.0174
	L	0.0386	0.0357	0.0714	0.00010	0.0207	0.0243
Sub 1	R	0.0590	0.0602	0.0990	0.00005	0.0307	0.0351
	L	0.0254	0.0277	0.0430	0.00048	0.0150	0.0203
Sub 2	R	0.0316	0.0255	0.0628	0.00130	0.0167	0.0144
	L	0.0557	0.0475	0.1120	0.00070	0.0295	0.0206
Sub 3	R	0.0422	0.0400	0.0737	0.00059	0.0230	0.0182
	L	0.0326	0.0292	0.0586	0.00013	0.0172	0.0120
Sub 4	R	0.0389	0.0402	0.0634	0.00420	0.0197	0.0307
	L	0.0408	0.0401	0.0674	0.00100	0.0191	0.0255
Sub 5	R	0.0258	0.0236	0.0506	0.00035	0.0145	0.0247
	L	0.0218	0.0203	0.0415	0.00022	0.0127	0.0191
Sub 6	R	0.0403	0.0420	0.0682	0.00056	0.0193	0.0211
	L	0.0306	0.0333	0.0512	0.00002	0.0158	0.0261
Sub 7	R	0.0627	0.0461	0.1439	0.00038	0.0349	0.0522
	L	0.0599	0.0574	0.1165	0.00190	0.0312	0.0437
Sub 8	R	0.0436	0.0393	0.0749	0.00010	0.0238	0.0247
	L	0.0457	0.0477	0.8130	0.00110	0.0228	0.0240
Sub 9	R	0.0400	0.0352	0.0820	0.00010	0.0203	0.0160
	L	0.0807	0.0795	0.1663	0.00060	0.0303	0.0243

Table 4.3.: Distance between the actual and planned trajectory for each subject in medium mode. R and L represents Right arm and Left arm. RMSE is the Root Mean Square Error.

Medium Mode		Mean error	Median error	Max error	Min error	RMSE	Fréchet distance
		(m)	(m)	(m)	(m)	(m)	(m)
Sub 0	R	0.0344	0.0586	0.0302	0.00004	0.0194	0.0233
	L	0.0423	0.0805	0.0381	0.00002	0.0222	0.0256
Sub 1	R	0.0328	0.0594	0.0341	0.00050	0.0181	0.0362
	L	0.0308	0.0544	0.0280	0.00033	0.0184	0.0525
Sub 2	R	0.0308	0.058	0.0270	0.00370	0.0165	0.0385
	L	0.0371	0.0614	0.0403	0.00010	0.0182	0.0183
Sub 3	R	0.0420	0.0805	0.0359	0.00013	0.0247	0.0171
	L	0.0335	0.0611	0.0319	0.00020	0.0180	0.0130
Sub 4	R	0.0540	0.0767	0.0516	0.03380	0.0323	0.0656
	L	0.0366	0.0733	0.0283	0.00014	0.0180	0.0231
Sub 5	R	0.0212	0.0498	0.0151	0.00010	0.0122	0.0238
	L	0.0241	0.0378	0.0257	0.00050	0.0136	0.0177
Sub 6	R	0.0344	0.0730	0.0250	0.00620	0.0191	0.0313
	L	0.0299	0.0590	0.0259	0.00023	0.0162	0.0173
Sub 7	R	0.0667	0.1352	0.0525	0.00560	0.0362	0.0539
	L	0.0553	0.1242	0.0390	0.00007	0.0304	0.0357
Sub 8	R	0.0428	0.0830	0.0342	0.00027	0.0232	0.0211
	L	0.0351	0.0606	0.0351	0.00090	0.0189	0.0300
Sub 9	R	0.0314	0.0728	0.0266	0.00008	0.0169	0.0233
	L	0.0226	0.0390	0.0246	0.00040	0.0129	0.0310

Table 4.4.: Distance between the actual and planned trajectory for each subject in hard mode. R and L represents Right arm and Left arm. RMSE is the Root Mean Square Error.

Hard Mode		Mean error	Median error	Max error	Min error	RMSE	Fréchet distance
		(m)	(m)	(m)	(m)	(m)	(m)
Sub 0	R	0.0320	0.0570	0.0305	0.00020	0.0157	0.0278
	L	0.0377	0.0619	0.0343	0.00003	0.0195	0.0324
Sub 1	R	0.0345	0.0616	0.0395	0.00007	0.0178	0.0211
	L	0.0196	0.0243	0.0214	0.00060	0.0106	0.0203
Sub 2	R	0.0685	0.1206	0.0745	0.00070	0.0341	0.0871
	L	0.0209	0.0389	0.0205	0.00460	0.0124	0.0219
Sub 3	R	0.0232	0.0392	0.0226	0.00050	0.0137	0.0123
	L	0.0357	0.0700	0.0361	0.00025	0.0218	0.0071
Sub 4	R	0.0284	0.0433	0.0310	0.00009	0.0149	0.0230
	L	0.0411	0.0729	0.0333	0.00020	0.0197	0.0250
Sub 5	R	0.0287	0.0449	0.0293	0.00006	0.0137	0.0215
	L	0.0131	0.0204	0.0134	0.00050	0.0096	0.0194
Sub 6	R	0.0389	0.0815	0.0359	0.00340	0.0211	0.0250
	L	0.0336	0.0621	0.0300	0.00008	0.0165	0.0083
Sub 7	R	0.0717	0.01612	0.0597	0.00030	0.0406	0.0385
	L	0.0343	0.0538	0.0379	0.00010	0.0168	0.0308
Sub 8	R	0.0490	0.0700	0.0550	0.00040	0.0244	0.0380
	L	0.0477	0.0880	0.0405	0.00007	0.0254	0.0242
Sub 9	R	0.0520	0.1030	0.0467	0.00050	0.0261	0.0186
	L	0.0279	0.0446	0.0297	0.00030	0.0138	0.0173

Table 4.5.: Mean error \pm standard deviation of trajectory for all the subjects.

		Mean error \pm std (m)
Easy mode	R	0.0424 \pm 0.011
	L	0.0432 \pm 0.018
Medium mode	R	0.0390 \pm 0.013
	L	0.0347 \pm 0.009
Hard mode	R	0.0427 \pm 0.011
	L	0.0312 \pm 0.016

From the results presented by Table 4.4. we can compare the mean error and standard deviation with respect to all subjects, in the three exercise modes. The largest mean error, comparing the left and right arms, is in the easy mode, with an overall value of 0.0428 ± 0.020 m. Instead, the medium mode has the smallest overall mean error with a value of 0.032 ± 0.011 m.

One detail to stress is the highest and lowest value between the mean error values in Tables 4.2., 4.3. and 4.4. On easy mode, the higher mean error is 0.0807 m and the lower is 0.0218 m. For what concern the medium mode, conversely, the higher value is 0.0667 m and the lower is 0.0212 m. The hard mode presents values as 0.0717m and 0.0196 m as higher and lower mean error.

From the study of the correlation factor between TCP force and trajectory, several results came out, represented in Table 4.5. ,4.6. and 4.7. for easy, medium, and hard mode respectively. The tables present 4 columns, each one with a corresponding correlation factor between two vectors. The first column expresses the results from the component on the X axis of the trajectory coordinates and the component on X axis of the TCP force. The same is true for the second column, but in this case is all about the Y axis. The third column presents results about the correlation on Z axis.

The fourth column, instead, express the value of the correlation factor analysed on the whole trajectory matrix (x, y, z components) and the whole TCP force (x, y, z, components).

Table 4.6.: Correlation factor between trajectory and TCP force during exercise in easy mode.

Easy Mode		Correlation factor	Correlation factor	Correlation factor	Correlation factor trajectory
		X axis	Y axis	Z axis	
Sub 0	R	-0.746	-0.947	0.154	-0.343
	L	-0.947	-0.872	-0.108	-0.536
Sub 1	R	-0.965	-0.955	0.499	-0.068
	L	0.864	-0.923	0.711	0.175
Sub 2	R	-0.936	-0.913	0.477	0.181
	L	-0.963	-0.994	-0.822	-0.439
Sub 3	R	0.043	-0.973	0.142	-0.789
	L	-0.967	-0.989	0.400	-0.310
Sub 4	R	-0.137	-0.963	0.699	-0.858
	L	-0.893	-0.858	0.816	-0.434
Sub 5	R	0.350	-0.954	-0.592	-0.851
	L	-0.959	-0.938	0.548	-0.348
Sub 6	R	-0.406	-0.916	0.263	-0.356
	L	-0.878	-0.981	0.880	-0.224
Sub 7	R	-0.480	-0.838	0.644	0.405
	L	-0.837	-0.755	0.185	0.193
Sub 8	R	-0.803	-0.990	0.940	-0.172
	L	-0.758	-0.952	0.627	-0.412
Sub 9	R	0.400	-0.900	-0.856	-0.580
	L	-0.891	-0.377	0.347	-0.238

Table 4.7.: Correlation factor between trajectory and TCP force during exercise in medium mode.

Medium Mode		Correlation factor	Correlation factor	Correlation factor	Correlation factor
		X axis	Y axis	Z axis	trajectory
Sub 0	R	-0.694	-0.916	0.805	-0.369
	L	-0.917	-0.859	0.807	-0.839
Sub 1	R	-0.929	-0.992	0.517	-0.107
	L	-0.918	-0.885	0.135	0.374
Sub 2	R	-0.738	-0.893	-0.478	-0.293
	L	-0.974	-0.940	-0.860	-0.471
Sub 3	R	0.375	-0.978	0.682	-0.674
	L	-0.965	-0.997	-0.047	-0.301
Sub 4	R	0.666	-0.980	0.714	-0.868
	L	-0.940	-0.926	0.837	-0.513
Sub 5	R	0.196	-0.977	0.195	-0.811
	L	-0.946	-0.958	0.624	-0.315
Sub 6	R	-0.682	-0.978	0.043	-0.559
	L	-0.905	-0.990	0.836	-0.237
Sub 7	R	-0.316	-0.904	0.2247	0.361
	L	-0.847	-0.637	0.431	0.176
Sub 8	R	-0.746	-0.978	0.876	-0.167
	L	-0.579	-0.938	0.921	-0.337
Sub 9	R	0.831	-0.953	-0.868	-0.647
	L	-0.903	-0.964	-0.815	-0.088

Table 4.8.: Correlation factor between trajectory and TCP force during exercise in hard mode.

Hard Mode		Correlation factor	Correlation factor	Correlation factor	Correlation factor trajectory
		X axis	Y axis	Z axis	
Sub 0	R	-0.563	-0.928	0.688	-0.296
	L	-0.245	-0.887	0.624	-0.058
Sub 1	R	-0.945	-0.899	0.883	0.141
	L	-0.983	-0.925	0.921	0.035
Sub 2	R	0.212	-0.403	-0.545	-0.166
	L	-0.949	-0.949	-0.826	-0.019
Sub 3	R	0.240	-0.990	0.569	-0.542
	L	-0.994	-0.990	-0.199	0.130
Sub 4	R	0.896	-0.976	0.503	-0.819
	L	-0.758	-0.854	0.748	-0.407
Sub 5	R	-0.316	-0.956	0.093	-0.642
	L	-0.961	-0.977	0.704	-0.347
Sub 6	R	-0.636	-0.978	0.126	-0.574
	L	-0.980	-0.993	0.849	0.025
Sub 7	R	0.721	-0.852	0.318	0.489
	L	-0.918	-0.969	0.299	0.440
Sub 8	R	-0.123	-0.883	0.702	-0.113
	L	-0.539	-0.959	0.726	-0.220
Sub 9	R	0.799	-0.684	-0.225	-0.192
	L	-0.629	-0.867	0.084	-0.475

4.2.2. Force results

This section presents the results of the force analysis recorded by the robot's TCP during various exercises. From Figures 4.15., 4.16. and 4.17. immediately below, it is possible to appreciate the development of forces with respect to the X, Y and Z axis, during an entire repetition of the exercise, in easy (Fig. 4.15.), medium (Fig. 4.16.) and hard (Fig. 4.17.) modes.

On Table 4.8, 4.9. and 4.10 there is the list of results from the mean value, the median value, the minimum value, and the maximum value of force recorded during all the exercise sessions of both right and left arm. From Table 4.11. it can be appreciated the values of the overall mean, median, minimum, and maximum value of force on all the subjects in the three modalities.

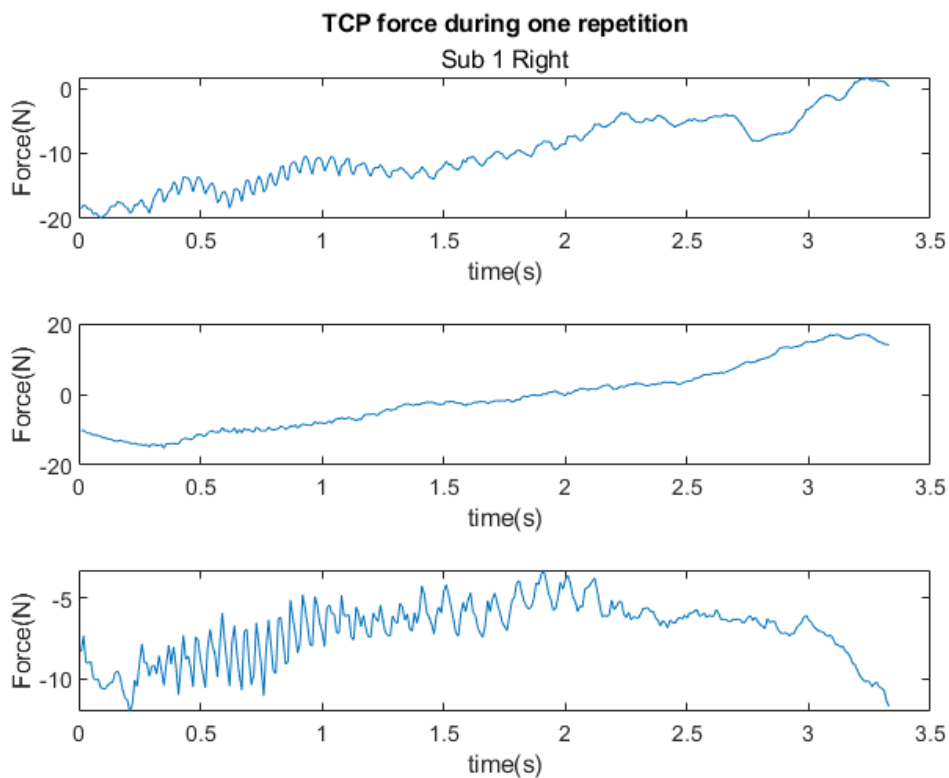


Figure 4.15.: TCP force recorded on X, Y and Z axis during one repetition in easy mode.

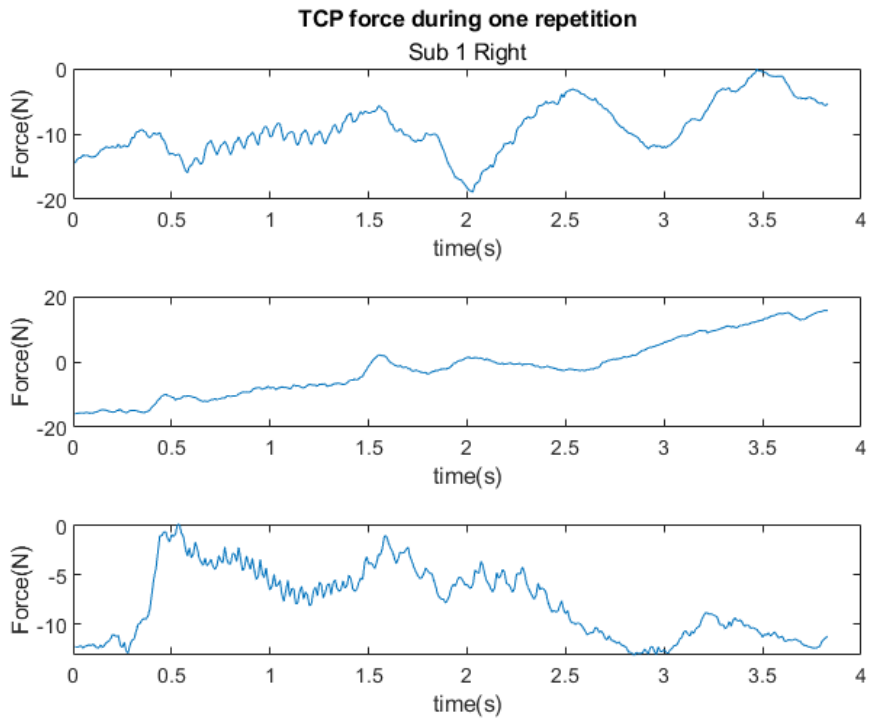


Figure 4.16.: TCP force recorded on X, Y and Z axis during one repetition in medium mode.

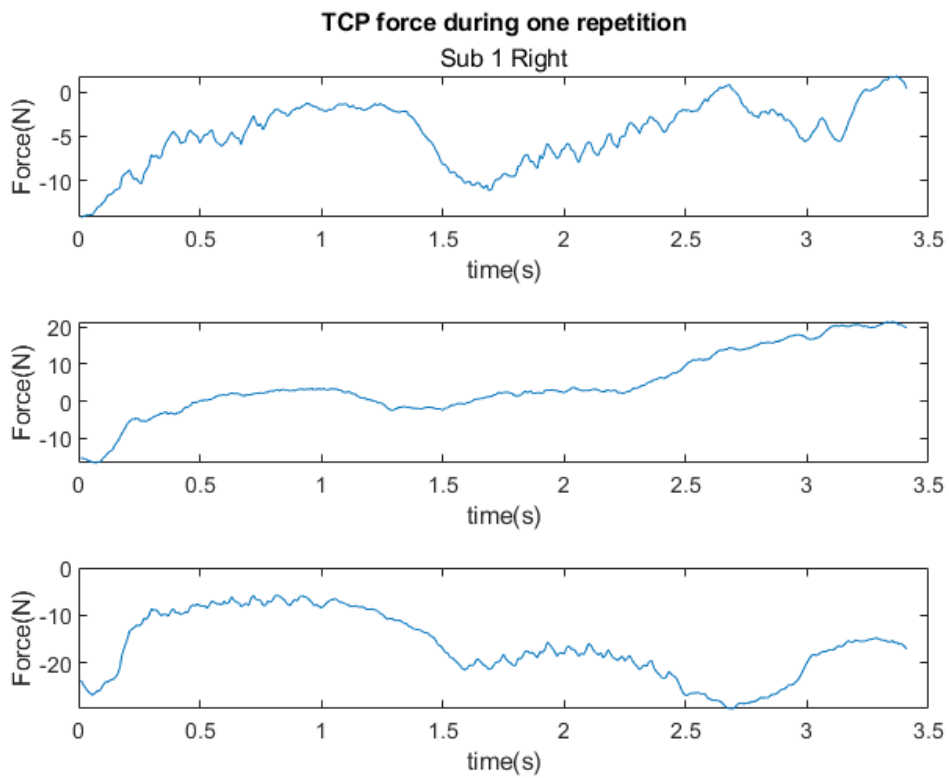


Figure 4.17.: TCP force recorded on X, Y and Z axis during one repetition in hard mode.

Table 4.9.: Results from the force analysis in easy mode. The force is analysed in its Mean, Median, Maximum and Minimum value.

Easy Mode		Mean force (N)	Median force (N)	Max force (N)	Min force (N)
Sub 0	R	8.06	6.48	20.16	3.58
	L	7.46	6.99	19.20	1.92
Sub 1	R	17.03	16.56	28.50	10.13
	L	14.34	14.30	20.60	9.57
Sub 2	R	9.16	9.60	13.29	5.37
	L	13.58	11.36	26.75	3.82
Sub 3	R	13.74	13.57	24.02	5.99
	L	11.30	10.57	21.58	3.01
Sub 4	R	17.05	17.37	23.82	10.01
	L	12.87	11.54	24.36	7.43
Sub 5	R	14.05	14.38	19.41	8.85
	L	11.16	9.63	23.40	3.17
Sub 6	R	7.23	7.54	9.54	4.03
	L	16.07	116.32	27.95	4.86
Sub 7	R	29.48	31.80	42.80	9.69
	L	19.61	19.56	37.79	4.61
Sub 8	R	24.61	25.77	37.91	11.29
	L	23.25	24.95	31.66	9.56
Sub 9	R	7.44	7.67	9.31	4.96
	L	9.06	11.77	17.20	0.44

Table 4.10.: Results from the force analysis in medium mode. The force is analysed in its Mean, Median, Maximum and Minimum value.

Medium Mode		Mean force (N)	Median force (N)	Max force (N)	Min force (N)
Sub 0	R	11.55	10.53	23.94	4.82
	L	8.72	8.99	15.06	3.32
Sub 1	R	26.58	25.59	33.28	17.19
	L	19.14	18.95	24.26	14.52
Sub 2	R	11.31	12.26	16.33	4.55
	L	13.24	12.72	22.18	5.05
Sub 3	R	19.71	17.64	33.40	9.65
	L	12.75	12.76	25.19	3.12
Sub 4	R	26.62	15.07	38.56	25.98
	L	16.27	9.62	22.17	16.34
Sub 5	R	18.35	10.91	24.38	18.52
	L	11.97	4.67	20.18	11.47
Sub 6	R	15.79	8.05	22.30	16.46
	L	14.28	5.112	29.47	13.17
Sub 7	R	42.15	20.51	55.29	44.46
	L	22.48	6.17	42.45	23.17
Sub 8	R	21.90	12.71	31.82	22.09
	L	26.86	12.90	35.77	28.02
Sub 9	R	9.89	6.27	13.28	9.65
	L	10.55	3.24	17.40	10.98

Table 4.11.: Results from the force analysis in hard mode. The force is analysed in its Mean, Median, Maximum and Minimum value.

Hard Mode		Mean force (N)	Median force (N)	Max force (N)	Min force (N)
Sub 0	R	10.50	9.85	16.98	5.31
	L	11.81	11.82	20.11	4.94
Sub 1	R	20.21	19.80	27.68	10.32
	L	11.65	11.50	17.09	5.69
Sub 2	R	15.34	12.01	36.46	4.47
	L	11.45	11.52	15.13	7.48
Sub 3	R	16.73	18.10	29.91	2.66
	L	13.09	14.14	22.95	4.17
Sub 4	R	27.14	30.39	43.78	10.82
	L	13.12	13.06	16.19	10.50
Sub 5	R	13.44	13.90	18.41	8.55
	L	8.13	7.712	14.58	2.23
Sub 6	R	15.98	16.49	22.30	8.05
	L	13.51	13.51	22.60	6.26
Sub 7	R	35.55	36.37	52.67	7.89
	L	18.90	18.11	25.50	8.37
Sub 8	R	19.79	20.82	25.53	7.68
	L	19.47	20.02	31.21	7.24
Sub 9	R	9.68	10.82	14.43	0.24
	L	5.40	5.79	9.03	1.80

Table 4.12.: Mean, Median, Minimum and Maximum force value and Standard Deviation on all subject in easy, medium, and hard mode.

		Mean force \pm std (N)	Median force \pm std (N)	Min force \pm std (N)	Max force \pm std (N)
Easy mode	R	14.78 \pm 7.55	13.98 \pm 8.30	3.58 \pm 2.88	42.80 \pm 11.21
	L	13.87 \pm 4.78	11.65 \pm 5.31	0.44 \pm 3.10	37.79 \pm 6.22
Medium mode	R	20.38 \pm 9.71	18.08 \pm 10.25	4.55 \pm 5.38	55.29 \pm 12.15
	L	15.64 \pm 5.65	13.06 \pm 6.02	3.12 \pm 4.14	42.45 \pm 8.40
Hard mode	R	18.44 \pm 7.87	17.28 \pm 8.62	0.24 \pm 3.38	52.67 \pm 12.30
	L	12.65 \pm 4.26	12.44 \pm 4.24	1.80 \pm 2.71	31.21 \pm 6.37

From the Table 4.11. results that the highest mean force recorded on all the subjects during the exercise is given by the right arm in the medium mode session, with a value of 20.38 \pm 9.71 N and a max force of 55.29 \pm 12.15 N.

On contrary, the lowest value is given by the left arm in hard mode, with a mean force of 12.65 \pm 4.26 N.

Chapter 5.

5.1. Discussion

The thesis aimed to develop an exercise for neuromuscular rehabilitation of the upper limb. The exercise was planned with peculiar characteristics that allow helping the subject to perform the task. One of the main features to follow is the robot assistance along a certain trajectory and, from the results, in paragraph 4.2.1. it can be appreciated that in every modality, during the whole exercise, the actual trajectory created by the subject has a similarity with the planned one. From Figure 4.10-11-12(a-b) it is possible to understand that, even if there is a certain variability, given by the freedom of movement of the control laws, the trajectory to reach the target is respected.

The three modalities developed with the exercise are planned to produce a force that helps or gives resistance to the subjects. From the trajectory results it can be established that the highest mean error is produced during the easy modality (0.0428 ± 0.02 m), this is probably due to the initial freedom given by the control law. Other factors can be the inexperience of the subjects to perform the exercise, and surely the variability due to the size, the force, and the mobility of all the subjects.

Observing the median error values from tables 4.1-4.2-4.3 it is observable a different behaviour from the mean. The value on all subjects in easy mode is 0.040 m, in medium mode 0.070 m and hard mode 0.059 m, having as the highest value in the medium mode.

Another peculiar feature of the exercise is based on the output force expressed by the robot on the subject. From the force analysis, it can be observed that the highest mean human force registered on the TCP during the exercise is produced in medium mode with a value of 20.38 ± 9.71 N on the right arm. The second highest mean force value belongs to the hard mode, and then the easy mode. From Table 4.8.-4.9. and 4.10. can be noticed that, compared to the rest, Subject 7 and Subject 8 impressed a mean force that is higher than all the other values, reaching a mean value in subject 7 during the exercise in medium mode with the right arm of 42.146 N and a max value of 55.29 N with the right and 42.45 N with the left arm.

Considering Subjects 7 and 8 as outliers, so excluding them from the results, the value of the mean forces impressed during the exercises in the three modalities is respectively, 11.85 N, 15.42 N and 14.00 N on easy, medium, and hard modes. The results are different looking at the more robust median of the TCP force. In this case, the values are 11.31 N, 11.40 N and 14.02 N in easy, medium, and hard modes.

Of course, these results are subjected to high variability. This is due to various factors, some of which have been listed before. An additional factor is psychological, where the subject expects that when changing modes, going from easiest to medium, there will be a greater increase in difficulty than there happens to be. Furthermore, other subjects did not respect the trajectory planned, increasing the resistance force produced by the control law and forcing the robot to counteract to maintain the trajectory, this leads to an increase in the TCP force registered.

A good point of discussion is based on the results of the correlation factor found between the trajectory and the TCP force during the experiments, where both are examined in their components. This analysis has the aim to find a correlation between the behaviour of the force with respect to the movement from start to target. In Table 4.5. the result in easy mode presents a strong inverse correlation between trajectory and force in X axis and Y axis components.

In easy mode the 100% of experiments the Y axis trajectory coordinate has a strong inverse correlation, with a mean of -0.899, instead, for the X axis 80% of the subjects present a quite strong inverse correlation, with a value of -0.545. For what concern the Z axis, it presents a low direct correlation in 80% of cases, with the value of 0.298.

In medium mode and in the hard mode the results are quite the same as for the easy mode. Also, the correlation factor between the whole trajectory coordinates and the components of the force has produced negative values in all the modalities, -0.300, -0.334 and -0.181 in easy, medium, and hard mode.

Of course, this correlation is based on trajectories planned on a fixed exercise framework. In this case it can be deduced that upon the subject's movement along the working area, as a response there is an inverse behaviour of the force. It can be concluded that, knowing that during the exercise the scalar force has a negative peak due to the coordinate frame, following the trajectory, the module of the force increase approaching the target. This behaviour is confirmed by the strong negative correlation with respect the Y axis, and by the negative correlation with respect all the components.

5.2. Conclusion

Collaborative robots arise as an evolution of industrial robots in terms of safety, lightweight, and programmability. These characteristics lead to the adoption of these robots not only for industrial applications but also in the medical field.

In the rehabilitation field, robot-aided rehabilitation is permanently increasing due to the many benefits that the cobot can give to the patient and the therapist. The high safety, lightweight and size of the cobots, added to the high precision, resistance and high repeatability allow the use of robots in the same environment as the patient, without any fear of being hurt by it. This thesis has aimed to develop a neuromuscular rehabilitation exercise for the upper limbs, that helps both the patient and the therapist during the rehabilitation therapy. As documented before, the work was divided into several stages, successfully completing each step of the process. from problem analysis to data acquisition. From the results, it is possible to appreciate the success of the aim of the thesis. It is evident the good performance of the control laws developed specifically for the success of this rehabilitation exercise. Regarding the exercise modalities, the force results produced by the data acquisition led to the conclusion that even if there is an increase in the resistance of robot to the reaching the target, this force could be increased, thus, increasing the proportionality at the base of the force produced by the robot it can be produced more resistance force.

The proposed framework can be improved in future works by increasing the resistance in the different modalities. Furthermore, could be introduced a different handle that has an active part of the rehabilitation for the fingers that allow an active assistive mode, using a mechanic glove.

Bibliography

- [1] J. E. Colgate, J. Edward, M. A. Peshkin, and W. Wannasuphprasit, “Cobots: Robots for collaboration with human operators,” 1996.
- [2] F. J. Hearl *et al.*, “Robotics in the Workplace,” *Patty’s Industrial Hygiene*, pp. 1–15, 2020, doi: 10.1002/0471435139.hygl40.
- [3] S. Haddadin and E. Croft, “Physical Human–Robot Interaction BT - Springer Handbook of Robotics,” B. Siciliano and O. Khatib, Eds. Cham: Springer International Publishing, 2016, pp. 1835–1874.
- [4] D. Kragic, J. Gustafson, H. Karaoguz, P. Jensfelt, and R. Krug, “Interactive, collaborative robots: Challenges and opportunities,” *IJCAI International Joint Conference on Artificial Intelligence*, vol. 2018-July, pp. 18–25, 2018, doi: 10.24963/ijcai.2018/3.
- [5] T. Lens, “Physical Human-Robot Interaction with a Lightweight, Elastic Tendon Driven Robotic Arm,” 2012.
- [6] A. De Santis, B. Siciliano, A. De Luca, and A. Bicchi, “An atlas of physical human-robot interaction,” *Mechanism and Machine Theory*, vol. 43, no. 3, pp. 253–270, 2008, doi: 10.1016/j.mechmachtheory.2007.03.003.
- [7] A. Carroll, “World report on disability,” *Irish Medical Journal*, vol. 105, no. 5, 2012, doi: 10.1111/j.1741-1130.2011.00320.x.
- [8] A. Cieza, K. Causey, K. Kamenov, S. W. Hanson, S. Chatterji, and T. Vos, “Global estimates of the need for rehabilitation based on the Global Burden of Disease study 2019: a systematic analysis for the Global Burden of Disease Study 2019,” *The Lancet*, vol. 396, no. 10267, pp. 2006–2017, 2020, doi: 10.1016/S0140-6736(20)32340-0.
- [9] Y. Béjot, H. Bailly, J. Durier, and M. Giroud, “Epidemiology of stroke in Europe and trends for the 21st century.,” *Presse medicale (Paris, France : 1983)*, vol. 45, no. 12 Pt 2, pp. e391–e398, Dec. 2016, doi: 10.1016/j.lpm.2016.10.003.
- [10] B. C. V Campbell *et al.*, “Ischaemic stroke,” *Nature Reviews Disease Primers*, vol. 5, no. 1, p. 70, 2019, doi: 10.1038/s41572-019-0118-8.
- [11] D. G. Kamper, H. C. Fischer, E. G. Cruz, and W. Z. Rymer, “Weakness is the primary contributor to finger impairment in chronic stroke.,” *Archives of physical medicine and rehabilitation*, vol. 87, no. 9, pp. 1262–1269, Sep. 2006, doi: 10.1016/j.apmr.2006.05.013.
- [12] G. Kwakkel, B. Kollen, and E. Lindeman, “Understanding the pattern of functional recovery after stroke: facts and theories.,” *Restorative neurology and neuroscience*, vol. 22, no. 3–5, pp. 281–299, 2004.
- [13] F. Buma, G. Kwakkel, and N. Ramsey, “Understanding upper limb recovery after stroke.,” *Restorative neurology and neuroscience*, vol. 31, no. 6, pp. 707–722, 2013, doi: 10.3233/RNN-130332.
- [14] H. Feys *et al.*, “Early and repetitive stimulation of the arm can substantially improve the long-term outcome after stroke: a 5-year follow-up study of a randomized trial.,” *Stroke*, vol. 35, no. 4, pp. 924–929, Apr. 2004, doi: 10.1161/01.STR.0000121645.44752.f7.

- [15] K. R. Lohse, C. E. Lang, and L. A. Boyd, "Is more better? Using metadata to explore dose-response relationships in stroke rehabilitation.," *Stroke*, vol. 45, no. 7, pp. 2053–2058, Jul. 2014, doi: 10.1161/STROKEAHA.114.004695.
- [16] J. van Kordelaar, E. van Wegen, and G. Kwakkel, "Impact of time on quality of motor control of the paretic upper limb after stroke.," *Archives of physical medicine and rehabilitation*, vol. 95, no. 2, pp. 338–344, Feb. 2014, doi: 10.1016/j.apmr.2013.10.006.
- [17] K. J. Waddell, R. L. Birkenmeier, J. L. Moore, T. G. Hornby, and C. E. Lang, "Feasibility of high-repetition, task-specific training for individuals with upper-extremity paresis.," *The American journal of occupational therapy : official publication of the American Occupational Therapy Association*, vol. 68, no. 4, pp. 444–453, 2014, doi: 10.5014/ajot.2014.011619.
- [18] T. Platz, "[Evidence-based arm rehabilitation--a systematic review of the literature].," *Der Nervenarzt*, vol. 74, no. 10, pp. 841–849, Oct. 2003, doi: 10.1007/s00115-003-1549-7.
- [19] R. Riener, T. Nef, and G. Colombo, "Robot-aided neurorehabilitation of the upper extremities.," *Medical & biological engineering & computing*, vol. 43, no. 1, pp. 2–10, Jan. 2005, doi: 10.1007/BF02345116.
- [20] T. Nef, M. Mihelj, G. Colombo, and R. Riener, "ARMin - Robot for rehabilitation of the upper extremities," *Proceedings - IEEE International Conference on Robotics and Automation*, vol. 2006, no. May, pp. 3152–3157, 2006, doi: 10.1109/ROBOT.2006.1642181.
- [21] S. C. Cramer and R. J. Nudo, *Brain repair after stroke*. Cambridge University Press, 2010.
- [22] E. Guglielmelli, M. J. Johnson, and T. Shibata, "Guest editorial special issue on rehabilitation robotics," *IEEE Transactions on Robotics*, vol. 25, no. 3, pp. 477–480, 2009.
- [23] A. Bowen, C. Hazelton, A. Pollock, and N. B. Lincoln, "Cognitive rehabilitation for spatial neglect following stroke," *Cochrane database of systematic reviews*, no. 7, 2013.
- [24] T. Hoffmann, S. Bennett, C.-L. Koh, and K. McKenna, "A systematic review of cognitive interventions to improve functional ability in people who have cognitive impairment following stroke," *Topics in stroke rehabilitation*, vol. 17, no. 2, pp. 99–107, 2010.
- [25] J. W. Krakauer, "Motor learning: its relevance to stroke recovery and neurorehabilitation.," *Current opinion in neurology*, vol. 19, no. 1, pp. 84–90, Feb. 2006, doi: 10.1097/01.wco.0000200544.29915.cc.
- [26] G. Kwakkel *et al.*, "Effects of augmented exercise therapy time after stroke: a meta-analysis," *stroke*, vol. 35, no. 11, pp. 2529–2539, 2004.
- [27] A. A. A. Timmermans, H. A. M. Seelen, R. D. Willmann, and H. Kingma, "Technology-assisted training of arm-hand skills in stroke: concepts on reacquisition of motor control and therapist guidelines for rehabilitation technology design," *Journal of neuroengineering and rehabilitation*, vol. 6, no. 1, pp. 1–18, 2009.
- [28] T. A. Jones, C. J. Chu, L. A. Grande, and A. D. Gregory, "Motor skills training enhances lesion-induced structural plasticity in the motor cortex of adult rats," *Journal of Neuroscience*, vol. 19, no. 22, pp. 10153–10163, 1999.
- [29] G. Kempermann, H. van Praag, and F. H. Gage, "Activity-dependent regulation of neuronal plasticity and self repair.," *Progress in brain research*, vol. 127, pp. 35–48, 2000, doi: 10.1016/s0079-6123(00)27004-0.

- [30] F. Gómez-Pinilla, Z. Ying, R. R. Roy, R. Molteni, and V. R. Edgerton, “Voluntary exercise induces a BDNF-mediated mechanism that promotes neuroplasticity.,” *Journal of neurophysiology*, vol. 88, no. 5, pp. 2187–2195, Nov. 2002, doi: 10.1152/jn.00152.2002.
- [31] R. J. Nudo and K. M. Friel, “Cortical plasticity after stroke: implications for rehabilitation.,” *Revue neurologique*, vol. 155, no. 9, pp. 713–717, 1999.
- [32] N. Tejima, “Rehabilitation robotics: a review,” *Advanced Robotics*, vol. 14, no. 7, pp. 551–564, 2001.
- [33] F. Badesa, R. Morales, J. M. Sabater-Navarro, N. Garcia-Aracil, J. M. Azorin, and C. Perez, “Experiencias en el desarrollo de un sistema robótico para rehabilitación de miembro superior para pacientes con daño cerebral sobrevenido,” *Revista Universitaria en Telecomunicaciones, Informática y Control*, vol. 1, no. 1, 2012.
- [34] A. Basteris, S. M. Nijenhuis, A. H. A. Stienen, J. H. Burke, G. B. Prange, and F. Amirabdollahian, “Training modalities in robot-mediated upper limb rehabilitation in stroke: a framework for classification based on a systematic review.,” *Journal of neuroengineering and rehabilitation*, vol. 11, p. 111, Jul. 2014, doi: 10.1186/1743-0003-11-111.
- [35] D. Lynch, M. Ferraro, J. Krol, C. M. Trudell, P. Christos, and B. T. Volpe, “Continuous passive motion improves shoulder joint integrity following stroke.,” *Clinical rehabilitation*, vol. 19, no. 6, pp. 594–599, Sep. 2005, doi: 10.1191/0269215505cr901oa.
- [36] C. Duret, A. G. Grosmaire, and H. I. Krebs, “Robot-assisted therapy in upper extremity hemiparesis: Overview of an evidence-based approach,” *Frontiers in Neurology*, vol. 10, no. APR, pp. 1–8, 2019, doi: 10.3389/fneur.2019.00412.
- [37] A. Majidrad, V. Adhikari, and Y. Yihun, “Assessment of Robot Interventions in a Task-based Rehabilitation: A case study,” *Proceedings of the Annual International Conference of the IEEE Engineering in Medicine and Biology Society, EMBS*, vol. 2018-July, pp. 1825–1828, 2018, doi: 10.1109/EMBC.2018.8512629.
- [38] L. de Azevedo Fernandes, T. Brito, L. Piardi, J. Lima, and P. Leitão, “A real framework to apply collaborative robots in upper limb rehabilitation,” *BIODEVICES 2020 - 13th International Conference on Biomedical Electronics and Devices, Proceedings; Part of 13th International Joint Conference on Biomedical Engineering Systems and Technologies, BIOSTEC 2020*, vol. 1, no. Biostec 2020, pp. 176–183, 2020, doi: 10.5220/0009004501760183.
- [39] M. L. Aisen, H. I. Krebs, N. Hogan, F. McDowell, and B. T. Volpe, “The effect of robot-assisted therapy and rehabilitative training on motor recovery following stroke.,” *Archives of neurology*, vol. 54, no. 4, pp. 443–446, Apr. 1997, doi: 10.1001/archneur.1997.00550160075019.
- [40] A. Toth, G. Fazekas, G. Arz, M. Jurak, and M. Horvath, “Passive robotic movement therapy of the spastic hemiparetic arm with REHAROB: report of the first clinical test and the follow-up system improvement,” in *9th International Conference on Rehabilitation Robotics, 2005. ICORR 2005.*, 2005, pp. 127–130.
- [41] E. D. Oña, J. M. Garcia-Haro, A. Jardón, and C. Balaguer, “Robotics in health care: Perspectives of robot-aided interventions in clinical practice for rehabilitation of upper limbs,” *Applied sciences*, vol. 9, no. 13, p. 2586, 2019.
- [42] P. S. Lum, C. G. Burgar, M. Van der Loos, P. C. Shor, M. Majmundar, and R. Yap, “MIME robotic device for upper-limb neurorehabilitation in subacute stroke subjects: A follow-up

study.,” *Journal of rehabilitation research and development*, vol. 43, no. 5, pp. 631–642, 2006, doi: 10.1682/jrrd.2005.02.0044.

- [43] C. Schmitt and P. Métrailler, “The Motion MakerTM: a rehabilitation system combining an orthosis with closed-loop electrical muscle stimulation,” in *8th Vienna international workshop on functional electrical stimulation*, 2004, no. CONF, pp. 117–120.
- [44] M. Bouri *et al.*, “The WalkTrainer: a robotic system for walking rehabilitation,” in *2006 IEEE International Conference on Robotics and Biomimetics*, 2006, pp. 1616–1621.
- [45] Y. Stauffer *et al.*, “The walktrainer—a new generation of walking reeducation device combining orthoses and muscle stimulation,” *IEEE Transactions on neural systems and rehabilitation engineering*, vol. 17, no. 1, pp. 38–45, 2008.
- [46] M. Bouri, B. Le Gall, and R. Clavel, “A new concept of parallel robot for rehabilitation and fitness: The Lambda,” *2009 IEEE International Conference on Robotics and Biomimetics, ROBIO 2009*, pp. 2503–2508, 2009, doi: 10.1109/ROBIO.2009.5420481.
- [47] M. Babaiasl, S. H. Mahdioun, P. Jaryani, and M. Yazdani, “A review of technological and clinical aspects of robot-aided rehabilitation of upper-extremity after stroke,” *Disability and Rehabilitation: Assistive Technology*, vol. 11, no. 4, pp. 263–280, 2016.
- [48] J. Mehrholz, A. Hädrich, T. Platz, J. Kugler, and M. Pohl, “Electromechanical and robot-assisted arm training for improving generic activities of daily living, arm function, and arm muscle strength after stroke,” *Cochrane database of systematic reviews*, no. 6, 2012.
- [49] D. H. Yoo and S. Y. Kim, “Effects of upper limb robot-assisted therapy in the rehabilitation of stroke patients,” *Journal of physical therapy science*, vol. 27, no. 3, pp. 677–679, 2015.
- [50] V. Klamroth-Marganska *et al.*, “Three-dimensional, task-specific robot therapy of the arm after stroke: a multicentre, parallel-group randomised trial,” *The Lancet Neurology*, vol. 13, no. 2, pp. 159–166, 2014.
- [51] M. Stefano, P. Patrizia, A. Mario, G. Ferlini, R. Rizzello, and G. Rosati, “Robotic upper limb rehabilitation after acute stroke by NeReBot: Evaluation of treatment costs,” *BioMed Research International*, vol. 2014, 2014, doi: 10.1155/2014/265634.
- [52] G. B. Prange *et al.*, “The effect of arm support combined with rehabilitation games on upper-extremity function in subacute stroke: a randomized controlled trial,” *Neurorehabilitation and neural repair*, vol. 29, no. 2, pp. 174–182, 2015.
- [53] E. Papaleo, L. Zollo, L. Spedaliere, and E. Guglielmelli, “Patient-tailored adaptive robotic system for upper-limb rehabilitation,” in *2013 IEEE International Conference on Robotics and Automation*, 2013, pp. 3860–3865.
- [54] J. M. Prendergast, S. Balvert, T. Driessen, A. Seth, and L. Peternel, “Biomechanics Aware Collaborative Robot System for Delivery of Safe Physical Therapy in Shoulder Rehabilitation,” *IEEE Robotics and Automation Letters*, vol. 6, no. 4, pp. 7177–7184, 2021, doi: 10.1109/LRA.2021.3097375.
- [55] G. Chiriatti, G. Palmieri, and M. C. Palpacelli, “A Framework for the Study of Human-Robot Collaboration in Rehabilitation Practices,” *Mechanisms and Machine Science*, vol. 84, no. June, pp. 190–198, 2020, doi: 10.1007/978-3-030-48989-2_21.
- [56] E. Kyrkjebø, M. Johan Laastad, and O. Stavdahl, “Feasibility of the UR5 Industrial Robot for Robotic Rehabilitation of the Upper Limbs After Stroke,” *IEEE International Conference on Intelligent Robots and Systems*, pp. 6124–6129, 2018, doi: 10.1109/IROS.2018.8594413.

- [57] Universal Robots, “Universal Robots e-Series User Manual,” pp. 1–119, 2018.
- [58] N. Enayati, E. De Momi, and G. Ferrigno, “Haptics in robot-assisted surgery: Challenges and benefits,” *IEEE Reviews in Biomedical Engineering*, vol. 9, pp. 49–65, 2016, doi: 10.1109/RBME.2016.2538080.
- [59] C. Schou, R. S. Andersen, D. Chrysostomou, S. Bøgh, and O. Madsen, “Skill-based instruction of collaborative robots in industrial settings,” *Robotics and Computer-Integrated Manufacturing*, vol. 53, no. March, pp. 72–80, 2018, doi: 10.1016/j.rcim.2018.03.008.
- [60] F. Domrös, D. Störkle, J. Ilmberger, and B. Kuhlenkötter, “A Motion Library for Robot-Based Upper Limb Rehabilitation BT - Converging Clinical and Engineering Research on Neurorehabilitation,” 2013, pp. 409–413.
- [61] A. S. Sørensen, T. R. Savarimuthu, J. Nielsen, and U. P. Schultz, “Towards using a generic robot as training partner: Off-the-shelf robots as a platform for flexible and affordable rehabilitation,” *ACM/IEEE International Conference on Human-Robot Interaction*, pp. 294–295, 2014, doi: 10.1145/2559636.2559842.
- [62] O. Rincón-Becerra and G. García-Acosta, “Estimation of anthropometric hand measurements using the ratio scaling method for the design of sewn gloves,” *DYNA (Colombia)*, vol. 87, no. 215, pp. 146–155, 2020, doi: 10.15446/dyna.v87n215.87984.

Appendix A.

A.1. Scripts used to program the UR5e

Script URSim:

Init Variables

Before start

```
zero_fsensor()
ciclo_0:=1
a:="Lunghezza tcp [m]"
```

Robot Program

```
programmi_script
script: f_robot_dipendente_f_human_new.script
script: 4_Laws.script
script: F_molla_distanza_new.script
script: F_molla_distanza_new.script
script: Cambio_Riferimento_new.script
target:=p[0,0,0,0,0,0]
```

Braccio DX o SX

```
braccio:='Braccio Destro o Sinistro? Destro = d; Sinistro = s'
if braccio = "d"
start:= p[0.664, 0.226, 0.100, 2.2, -2.2, 0]
elseif braccio = "s"
start:= p[0.664, -0.273, 0.100, 2.232, -2.21, 0]
elseif braccio != "d" or braccio != "s"
Popup: Parametro errato
MoveL
start
Setup Force mode
tipo:= 'Modalità di esercizio? facile = f medio = m difficile = d'
perc:=[0.5,0,0.5]
if tipo = "f"
damp_esercizio:= 0.003
elseif tipo = "m"
damp_esercizio:= 0.003
elseif tipo = "d"
damp_esercizio:= 0.003
else
Popup: Modalità errata
Loop inizio_prog = False
inizio_prog :='Posizionare il target nell'area di lavoro. Fatto?'
```

```

ripetizione:= 'Quante volte ripetere l'esercizio?'
if ciclo_0 = 1
start_point:= get_actual_tcp_pose()
start_point
freedrive_mode(freeAxes=[1,1,1,0,0,1], feature = p[0,0,0,0,0,0])
scelta:= 'Set up completato?'
if scelta = True
end_freedrive_mode()
inizio_sx:= get_actual_tcp_pose()
inizio_sx_hand:= hand_pose
inizio_sx
timer_1: Start
calib_f:=0
Suono_1
Set DO[3] = On
Wait: 0.1
Set DO[3] = Off
Wait: 1.0
n_misure:=0

```

Procedura Peso braccio

```

Wait: 3.0
Loop timer_1<5
Calib_f:= calib_f+force()
N_misure := n_misure +1
Wait: 0.1
Calib_f:= (calib_f/n_misure)*1.2
Timer_1 : Stop
Timer_1 :=0
Suono_1
Set DO[3] = On
Wait: 0.1
Set DO[3] = Off
Wait: 1.0
Timer_1: Start
F_massima :=0

```

Procedura per la forza massima del paziente

```

Wait: 3.0
Loop timer_1 < 3
F_act := force()
If f_act > f_massima
F_massima:= f_act
Wait: 0.1

```

```

Timer_1: Stop
Timer_1:= 0
Ciclo_0 := 0
MoveL
Inizio_x
Suono_2
Set DO[3] = On
Wait: 0.25
Set DO[3] = Off
Wait: 0.25
Set DO[3] = On
Wait: 0.25
Set DO[3] = Off
Wait: 0.25
Esercizio_on := 0
Loop ripetizione != 0
Loop digital_out[3] != True
Ori:= change_orientation(inizio_sx_hand,target)
C_h_v:=get_tcp_force()
C_h:= C_h_v[5]
F_vera_Lin := f_robot_dipendente(f_massima,tipa,target,ori,perc)
F_r_molla := f_molla(posa_tcp_ini,ori,target,inizio_sx,hand_pose)
Tcp := get_actual_tcp_pose()
Flange_t := get_actual_tool_flange_pose()
C_r := Cr_gain4(C_h,3,0.97,0.03)
C_r_1 :=C_robot(C_h,5)
Force_mode(p[tcp[0],tcp[1]tcp[2],0,0,0],[1,1,1,0,0,1],[F_r_molla[0]+F_vera_Lin[0],
F_r_molla[1]+F_vera_Lin[1], F_r_molla[2]+F_vera_Lin[2],0,0,C_r_1[0]
,2,[1,1,1,0.785,0.785,0.785]])
If (force())>calib_f*0.9)
Force_mode_set_damping(damp_esercizio)
Esercizio_on :=1
Elseif esercizio_on := 0
Force_mode_set_damping(1)
Force_mode(p[tcp[0],tcp[1]tcp[2],0,0,0],[0,0,0,0,0,0],[F_r_molla[0]+F_vera_Lin[0],
F_r_molla[1]+F_vera_Lin[1], F_r_molla[2]+F_vera_Lin[2],0,0,C_r_1[0]
,2,[1,1,1,0.785,0.785,0.785]])
Sync()
End_force_mode()
Esercizio_on := 0
Ripetizione := ripetizione -1
If ripetizione != 0
MoveL
Tcp_pose := get_actual_tcp_pose()

```

Tcp_pose
Wait: 0.5
Inizio_sx

Suono_2

Set DO[3] = On
Wait: 0.25
Set DO[3] = Off
Wait: 0.25
Set DO[3] = On
Wait: 0.25
Set DO[3] = Off
Wait: 0.25
Else
P_alto_1 := get_actual_tcp_pose()
P_alto_1
Inizio_sx

Suono 3

Set DO[3] = On
Wait: 0.25
Set DO[3] = Off
Wait: 0.25
Set DO[3] = On
Wait: 0.25
Set DO[3] = Off
Wait: 0.25
Set DO[3] = On
Wait: 0.25
Set DO[3] = Off
Wait: 0.25

Thread_1

Wait:0.01
Missing: Cognex Camera Pose
X_target := CG_result [0]
Y_target := CG_result [1]
Target_act := p[X_target, Y_target, -0.01, 2.22, -2.22, 0]
Hand_pose := pose_trans (get_actual_tcp_pose(),p[0,a,0,0,0,0])
If inizio_program = True
Target:= target_act
Inizio_prog := False
Missing : job Pass
Missing:No response

Popup: no response

Thread_2

Wait: 0.01

Posa_tacp_ini := get_actual_tcp_pose()

Diff := point_dist(hand_pose,target)

If diff < 0.025

Wait: 0.5

Set DO[3] = On

Wait: 0.25

Set DO[3] = Off

Wait: 1

Script 'f_robot_dipendente_f_human_new.script'

Def f_robot_dipendente(f_massima, tipo, target, ori, perc):

#Calcolo f_uomo

F_vera = get_tcp_force()

F_vera_Lin = pose_trans(pose_inv(p[target[0],target[1],target[2],ori[0],ori[1],ori[2]]),F_vera)

#modalità facile: 20% della f_vera forza uomo percepita

#modalità media: 50% della f_vera forza uomo percepita

#modalità difficile: 90% della f_vera forza uomo percepita

If tipo == "f":

*F_vera_Lin = p[0,0,F_vera_Lin[2]*perc[0],0,0,0]*

Elif tipo == "m":

*F_vera_Lin = p[0,0,F_vera_Lin[2]*perc[1],0,0,0]*

Elif tipo == "d":

*F_vera_Lin = p[0,0,F_vera_Lin[2]*perc[2],0,0,0]*

End

F_vera_Lin = pose_trans(p[0,0,0,ori[0],ori[1],ori[2]], F_vera_Lin)

Return F_vera_Lin

end

Script "4_Laws"

Def Cr_gain4(C_h,a,b,c):

X = C_h

If norm(x) <= c:

Cr = 0

Elif norm(x) > c and norm(x) <= 1:

Cr = 3(a/pow(b,2))*pow(norm(x)-c,2)-(2*a/pow(b,3))*pow(norm(x)-c,3)*

*Cr = Cr*x/norm(x)*

Elif norm(x) >= 1:

Cr = a

*Cr = Cr*x/norm(x)*

End
 Return [Cr,x]
 End

Script “Control_law”

```

Def C_robot(C_h,C_0):
X = C_h/C_0
If x<=-1:
Cr = 0
Elif x>=1:
Cr = 0
Elif x>= -0.1 and x<=0:
Cr = 147.353*pow(x,3)- 0.431*pow(x,2)
Elif x>-0.25 and x<=-0.1:
Cr =-164.6064*pow(x,3)- 70.621*pow(x,2)- 4.679317*x - 0.077988
Elif x>-0.275 and x<=-0.25:
Cr =885.4342*pow(x,3)+ 716.9098*pow(x,2)+19.2035*x +16.32891
Elif x>-0.3 and x<=-0.275:
Cr =-200.4389*pow(x,3)- 178.9355*pow(x,2)+54.154*x -0.687
Elif x>-0.4 and x<=-0.3:
Cr =5.716*pow(x,3)+ 6.6 *pow(x,2)+1.508*x +16.32891
Elif x>-0.5 and x<=-0.4:
Cr =0.608*pow(x,3)+ 0.4745*pow(x,2)+0.9439*x -1.0145
Elif x>-0.7 and x<=-0.5:
Cr =-3.132*pow(x,3) -5.136*pow(x,2)-3.749*x -1.482
Elif x>-0.75 and x<=-0.7:
Cr =14.0245*pow(x,3)+ 30.892*pow(x,2)+21.471*x -4.402
Elif x>-0.8 and x<=-0.75:
Cr =-12.467*pow(x,3) -28.7135*pow(x,2)-23.233*x -6.77
Elif x>-1 and x<=-0.8:
Cr =14.269*pow(x,3)+ 35.4545*pow(x,2)+28.101*x +6.915
Elif x>0 and x<=0.1:
Cr =147.353*pow(x,3)+ 0.431*pow(x,2)
Elif x>0.1 and x<=0.25:
Cr =-164.60*pow(x,3)+ 70.62*pow(x,2)-4.679*x +0.07
Elif x>0.25 and x<=0.275:
Cr =885.4342*pow(x,3)- 716.9098*pow(x,2)+192.2035*x -16.3289
Elif x>0.275 and x<=0.3:
Cr =-200.4389*pow(x,3)+ 178.9355*pow(x,2)-54.154*x +6.253
Elif x>0.3 and x<=0.4:
Cr =5.716*pow(x,3)- 6.604*pow(x,2)+1.508*x +0 .687
Elif x>0.4 and x<=0.5:
Cr =0.608*pow(x,3)- 0.4745*pow(x,2)+0.9439*x +1.0145
Elif x>0.5 and x<=0.7:

```

```

Cr = -3.13*pow(x,3)+ 5.136*pow(x,2)-3.749*x +1.482
Elif x>0.7 and x<=0.75:
Cr = 14.024*pow(x,3)-30.89*pow(x,2)+21.47*x -4.402
Elif x>0.75 and x<=0.8:
Cr = -12.267*pow(x,3)+ 28.71*pow(x,2)-23.23*x +6.77
Else:
Cr = 14.269*pow(x,3)- 35.4545*pow(x,2)+28.1*x -6.9155
End
Cr = C_0*Cr

```

```

Return [Cr,x]
end

```

Script “F_molla_distanza_new”

```

Def f_molla(posa_tcp_ini,ori,target,inizio_sx,hand_pose):
pose_tcp = get_actual_tcp_pose()
d_max = point_dist(hand_pose,target)
r_max = d_max/5
d_ori = pose_trans(pose_inv(p[target[0],target[1],target[2],ori[0],ori[1],ori[2]]),hand_pose)
d = sqrt(d_ori[2]*d_ori[2])
r = sqrt(d_ori[0]*d_ori[0]+d_ori[1]*d_ori[1])
m = d_max/r_max
r_0 = (1/m)*d
k_f = 2000
if r<r_0:
k = ((-k_f*r*r)/(r_0*r_0*r_0))*(2*r-3*r_0)
else:
k = k_f
end
F_r_opposta_x = -k*d_ori[0]
F_r_opposta_y = -k*d_ori[1]
F_r_opposta_z = -k*d_ori[2]*0
F_tot = [F_r_opposta_x, F_r_opposta_y, F_r_opposta_z]
F_tot0 = pose_trans(p[0,0,0,ori[0],ori[1],ori[2]],p[F_r_opposta_x, F_r_opposta_y,
F_r_opposta_z,0,0,0])
F_r_opposta_x = F_tot0[0]
F_r_opposta_y = F_tot0[1]
F_r_opposta_z = F_tot0[2]
Return [F_r_opposta_x, F_r_opposta_y, F_r_opposta_z,d_ori[0],d_ori[1],d_ori[2]]
end

```

